UNIVERSIDAD DE INVESTIGACIÓN DE TECNOLOGÍA EXPERIMENTAL YACHAY

Escuela de Ciencias Biológicas e Ingeniería

TÍTULO: Analysis of ultraviolet solar radiation in the generation of ocular pathology

Trabajo de integración curricular presentado como requisito para la obtención del título de Ingeniera Biomédica

Autor:

Fabian Rodrigo Cushcagua Arias

Tutor:

MSc. Paula Sofia Rodriguez Ormaza

Urcuquí, marzo del 2023

AUTORÍA

Yo, **Fabian Rodrigo Cushcagua Arias**, con cédula de identidad 1003878723, declaro que las ideas, juicios, valoraciones, interpretaciones, consultas bibliográficas, definiciones y conceptualizaciones expuestas en el presente trabajo; así cómo, los procedimientos y herramientas utilizadas en el presente trabajo, son de absoluta responsabilidad de el/la autora (a) del trabajo de integración curricular. Así mismo, me acojo a los reglamentos internos de la Universidad de Investigación de Tecnología Experimental Yachay.

Urcuquí, marzo del 2023.

Fabian Rodrigo Cushcagua Arias

CI: 1003878723

AUTORIZACIÓN DE PUBLICACIÓN

Yo, **Fabian Rodrigo Cushcagua Arias,** con cédula de identidad 1003878723, cedo a la Universidad de Investigación de Tecnología Experimental Yachay, los derechos de publicación de la presente obra, sin que deba haber un reconocimiento económico por este concepto. Declaro además que el texto del presente trabajo de titulación no podrá ser cedido a ninguna empresa editorial para su publicación u otros fines, sin contar previamente con la autorización escrita de la Universidad.

Asimismo, autorizo a la Universidad que realice la digitalización y publicación de este trabajo de integración curricular en el repositorio virtual, de conformidad a lo dispuesto en el Art. 144 de la Ley Orgánica de Educación Superior

Urcuquí, marzo del 2023.

Fabian Rodrigo Cushcagua Arias

CI: 1003878723

ABSTRACT

Ultraviolet solar radiation can cause minor problems in the eyes, but which can cause vision loss. Specifically, ultraviolet solar radiation is associated in the generation of pathologies such as cataract, pterygium, and corneal sunburn and they are generated due to longer exposure of ultraviolet rays to the eyes, which are caused by not using adequate protection such as glasses.

The UV radiation analysis will be carried out in the city of Otavalo-Imbabura located in northern Ecuador; due to the geographical location at more than 2000 meters above sea level, the solar radiation will be higher than coastal cities. An analysis of the protection used in this area will also be carried out, which should be greater than that used in places close to sea level.

In conclusion, this graduation project will determine the UV solar energy in the Otavalo zone and will analyze the generation of ocular pathologies produced by this UV exposure. In addition, the proper eye protection will be determined.

Keywords: Vision, electromagnetic spectrum, eye diseases, ultraviolet radiation, sun protection.

RESUMEN

La radiación solar ultravioleta puede causar problemas menores en los ojos, pero que pueden causar pérdida de la visión. En concreto, la radiación solar ultravioleta se asocia en la generación de patologías como cataratas, pterigión y quemaduras solares de la córnea y se generan por una mayor exposición de los rayos ultravioleta a los ojos, que se producen por no utilizar una protección adecuada como las gafas.

El análisis de radiación UV se realizará en la ciudad de Otavalo-Imbabura ubicada en el norte de Ecuador; Debido a la ubicación geográfica a más de 2000 metros sobre el nivel del mar, la radiación solar será mayor que la de las ciudades costeras. También se realizará un análisis de la protección utilizada en esta zona, que deberá ser mayor que la utilizada en lugares cercanos al nivel del mar.

En conclusión, este proyecto de graduación determinará la energía solar UV en la zona de Otavalo y analizará la generación de patologías oculares producidas por esta exposición a los rayos UV. Además, se determinará la protección ocular adecuada.

Palabras claves: Visión, espectro electromagnético, enfermedades del ojo, radiación ultravioleta, protección solar.

Agradecimientos

Quiero agradecer a la Universidad “Yachay Tech” por haberme brindado la oportunidad de demostrar mis habilidades, por dejarme formar de esta gran familia. Agradecer a todos los y las docentes por la disposición de brindar conocimiento durante todos estos años, por sus grandes consejos y por todo lo que se ha compartido.

A Graciela Salum Quiero de agradecerle de la manera más cordial por la paciencia y su manera de enseñar, por todos esos conocimientos académicos que me ha dado, pero sobre todo porque no solo me enseñó a desenvolverme como un estudiante sino como un ser humano.

Quiero reconocer a mis compañeros y amigos José, Jazz y Vane que estuvieron con su apoyo de todas las formas posibles, en las buenas y en las malas. A mis amigos de casa por sus contagiosas maneras de estudiar, a mis amigos de entretenimiento que durante todo este tiempo no han dejado de apoyarme y que enfermedades como el estrés y la depresión puedan alcanzarme, gracias amigos de baile: Hypnotic, Allpha Squad y G-Gravity.

Y finalmente a mi familia, que es lo más importante e incondicional que tengo a ellos me gustaría saber cómo agradecerles por todo lo que han hecho, quiero dar las gracias a mis padres y a mi hermana por los largos años de apoyo sin cansancio que me han regalado, por el esfuerzo de mantenerme estudiando, por su motivación constante y por todo el amor que me han obsequiado.

Dedicatoria

Para mi familia en especial para mi madre María Arias, mi padre José Cushcagua y mi hermana Belén Cushcagua que me han apoyado desde el inicio de mi carrera. Para mis amigos que me han sabido apoyar en las buenas y en las malas.

Table of Contents

List of Tables

List of Figures

1 INTRODUCTION

While exposure to the sun is beneficial to our health, such as the generation of vitamin D, but can also be dangerous since it can cause problems such as cancer. Prolonged exposure to solar radiation has been shown to cause eye problems; therefore, the eye can suffer from ocular pathologies due to exposure to solar radiation.

The eye is a wonder of nature due to its high complexity and fragility. However, at the same time, it fulfills unique functions such as vision, which has been crucial in the development of human society. This complex organ called the eye is made up of 3 main parts. The eye is exposed to free movement so that it can suffer irreparable damage from solar radiation. Its repair can be complicated, so care must be taken when carrying out any activity in full sunlight.

The solar radiation that reaches planet earth can be in different spectrums such as: ultraviolet spectrum, the visible spectrum, and the infrared. Solar radiation ranges from 100 to 400 corresponds to the spectrum of ultraviolet radiation, which is divided into type C from 100 nm to 280 nm, B from 280 nm to 315 nm, and A from 315 nm to 400 nm (Karam & Rojas, 2017).

The most damaging spectra for humans are ultraviolet radiation, which is more significant when several factors are met, such as greater visibility, such as high altitude, high albedo, clouds, and solar noon (Rivas & Rojas, 2018). Clouds play a fundamental role in tropical areas since they are associated with the distribution of water and heat and are also important in the temperature and radiation of the earth, depending on their behavior with each other and with large-scale circulations (Bony et al., 2015).

Aside from these visible factors, other elements can contribute to the damaging effect of ultraviolet radiation that cannot be seen with the naked eye, such as ozone levels and aerosols in the atmosphere. Ultraviolet radiation can cause damage, such as burns to the skin, but it can also cause damage to the eye system. The most common ocular pathologies caused by ultraviolet b radiation are cataracts, photoconjunctivitis, photokeratitis, and pterygium, although they can also be caused by artificial sources of ultraviolet c radiation (Garźon-Chaveza et al., 2018).

Throughout the year, the earth receives a significant amount of solar radiation, and several models have been created to understand the levels of irradiance. One is the TUV model, a web interface capable of performing calculations by filling in specific parameters that can affect solar radiation, such as those mentioned before (Mcneill, 2019).

Finally, solar radiation is beneficial for the proper development of the human being. However, suppose appropriate precautions are not taken. In that case, solar radiation can significantly harm the visual system, which can be a serious concern as some of these damages are irreversible. To avoid this, wearing hats and sunglasses with UV protection is recommended.

1.1 Eyes and vision

1.1.1 Anatomy and physiology of eyes

The visual function of fixing an image either at a short distance or a long distance involves two parts. The first is that the eyeball has to move until the captured image can be in the fovea of both eyes. The second is that the lens has to change power to make the image sharper (Cholewiak & Banks, 2019). A standard SLR camera follows the structure of the eye functions the primary function of the eye is vision, but to understand what vision is, it is necessary to know what the look is. The human eye consists of different parts, but there are three main ones.

The first section, which is the eye's outermost layer, can find the following parts: Clear cornea, Sclera, Opaque, limbo, Etc.

One of the essential parts of the eye's outermost layer is the cornea, which is avascular, in addition to balancing angiogenic and anti-angiogenic signals, allowing it to have the immunological privilege. If the cornea suffers any injury, it runs the risk of forming corneal neovascularization, which fills the stroma with liquids, thus making it difficult to see and could lead to loss of sight (Y. Wang & Chodosh, 2019).

In the second section is the middle uveal layer of the eye, the following parts: the iris, ciliary body, and choroid.

The iris is composed of 4 layers, starting from the lowest, the anterior border layer, the stroma, anterior epithelium, posterior epithelium, the iris has a circular structure which helps the optical system as it functions as a diaphragm. For its part, the ciliary body tends to be highly vascularized and is divided into 2 parts which are: the pars plicata and the relatively flat pars plana. The choroid plays an important role as it is in charge of exchanging catabolites with the retina, as well as providing the necessary nutrients to the outer retina (Tkachev et al., 2020).

The third section is the inner layer of the eye, better known as the retina.

The retina is a part, but it is not uniform. In the center is the macula, which is usually divided into sub-areas in the exact center, but with fewer photoreceptors; therefore, in those areas, the vision tends to be poor (Cholewiak & Banks, 2019). The retina can be damaged over the years, implying the photoreceptors' death. Factors such as tobacco can accelerate the damage of the retina and cause phrenopathy. One of the leading causes of retinal damage is light, as it can damage the outer segments of the photoreceptors (Jaadane et al., 2015).

To conclude, the human eye is very complex since it consists of the eye's outermost layer, which has several parts such as clear cornea, sclera, opaque, limbus, Etc. The cornea is essential as it balances angiogenic and anti-angiogenic signals. On the other hand, the middle uveal layer of the eye is also divided into the iris, ciliary body, and choroid. Furthermore, each of these is important for the proper functioning of the eye. Moreover, to finish, the inner layer of the eye or retina fulfills an essential function as it is the carrier of the photoreceptors necessary to capture light and different colors.

1.1.2 Vision: optical system and retina

The human being can have a coherent perception of what is around us, which is essentially thanks to the biological measurements of the eye's light (Brainard, 2015). Two photoreceptors are in charge of our vision: the rods and the cones. Although the cones' most significant light uptake occurs, they constitute only 5% of the retinal photoreceptors. In comparison, the rods receiving dim light make up nearly 95% of retinal photoreceptors (Lamb, 2016). Three subclasses of cones encode the different wavelengths that the eye can capture: for high-length light waves, they are encoded by L cones, encoded short length light by S cones, and for medium-wavelength light, the

M cones (Benson, Manning, & Brainard, 2014). The L and M cones can be associated with chromatic signaling and are associated with the sensation of red and green colors (Sabesan, Schmidt, Tuten, & Roorda, 2016). The ipRGC is considered a third photoreceptor, responsible for producing melanomas and capturing photons through the retinal chromophore attached to its protein part. However, they are also known as functions extra visual because they are not clearly related in image formation, such as rods and cones (Augusto & Jorge, 2015).

1.2 Solar radiation

Solar radiation is produced by the Sun, and the frequency range of solar electromagnetic radiation gives; as a result, the solar electromagnetic spectrum. The solar electromagnetic spectrum is formed by all electromagnetic waves in all energy ranges: gamma ray, x-ray, ultraviolet radiation, visible radiation, infrared radiation, microwaves, and radiofrequency radiation, named by highest energy and lowest energy.

All these types of radiation are produced by a fusion process in the Sun's core. Then, the solar radiation travels to the photosphere, which is the visible layer of the Sun from the Earth.

In this way, the solar radiation ranges that reach the terrestrial surface are part of ultraviolet, visible, and infrared radiation; this ranges from about 290 nm to 3000 nm.

1.2.1 Solar irradiance and spectral solar irradiance

The power measurement is called ***irradiance,*** and its unit is Watt (W). It is very usual to give the solar radiation in terms of the power per unit area, then the unit of irradiance is [W/m2] [11].

Figure 1

Solar spectral irradiances of sunlight without atmospheric absorption, ideal blackbody and sunlight at sea level

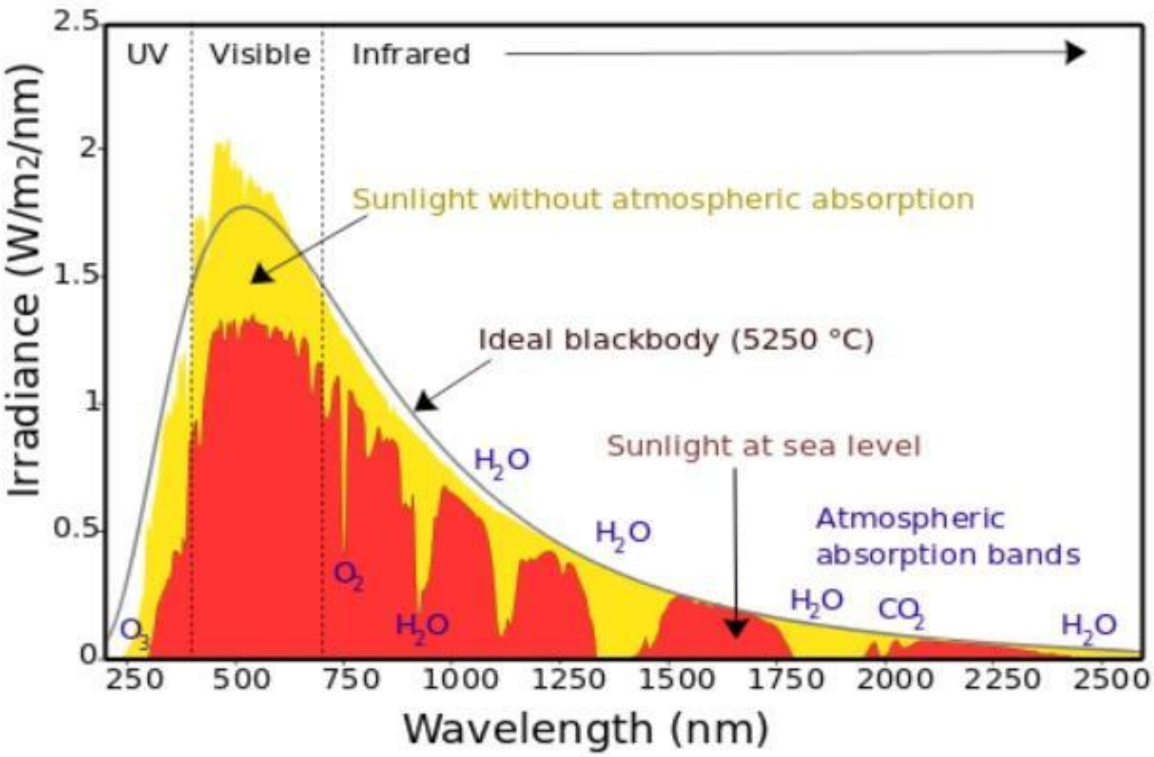

Taken from (PennState CEMS web page).

Figure 1 shows the ***spectral solar irradiance,*** which is the solar irradiance intensity per wavelength. The figure shows that the peak of solar radiation is in the visible range (PennState CEMS website).

Solar radiation reaches the terrestrial surface and then goes through the different layers of the atmosphere. Different atmospheric compounds attenuate different ranges of radiation. For example, the ozone gas attenuates the higher energy ultraviolet range in the stratospheric layer.

Figure 1 shows each window related to the gases: O3, H2O, O2, CO2, Etc. It is easy to see the relationship between the wavelength and the attenuated radiation and the fact that ozone is responsible for ultraviolet attenuation.

The sun produces radiation across various frequencies, including X-rays and radio waves. However, most solar radiation is concentrated in the visible light range. The typical units used to measure irradiance are Joules per second per square meter of surface area per wavelength interval. These units are used to measure the amount of radiation at a specific wavelength, known as spectral irradiance or irradiance, depending on the wavelength. In order to calculate the overall amount of irradiance measured in W m–2, the irradiance at each wavelength should be integrated.

1.2.2 Total, direct and diffuse solar radiation

Total (or global) solar radiation is the total solar radiation that reaches the terrestrial surface (about 290 nm to 3 µm). Also, total solar radiation is composed by (see Figure 2):

- Direct solar radiation: these are the photons that come directly from the Sun and are not absorbed or scattered when they pass through the atmosphere;

- Diffuse solar radiation: it is originated from the interaction between the photons with the matter of the atmosphere (Cabrera et al., 2005).

Figure 2

Diagram of direct and diffuse components of total solar

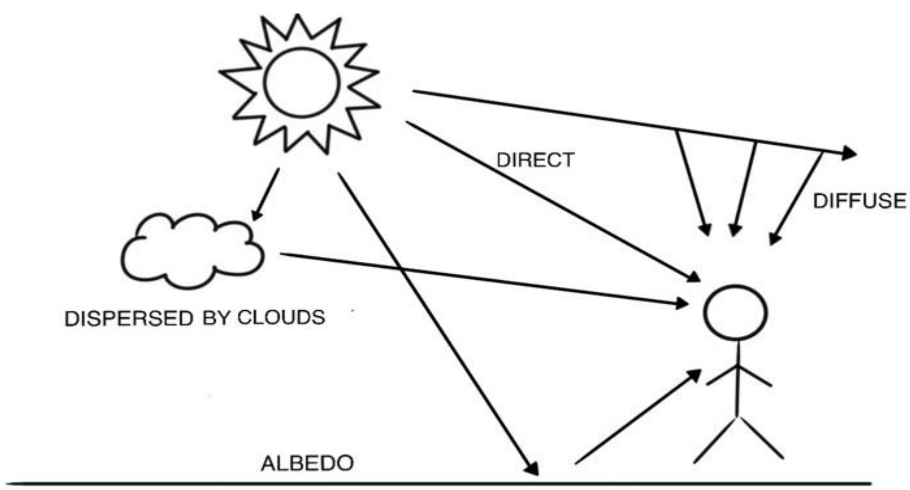

Adapted from (Cabrera et al., 2005).

1.2.3 Ultraviolet solar radiation

Solar ultraviolet radiation (UVR) is electromagnetic radiation with wavelengths from about 400 nm to 100 nm. UVR can be divided into three ranges:

- UVA: 315 to 400 nm. This range produces skin aging.
- UVB: 280 to 315 nm. This range of UVR produces skin burning.
- UVC: 200 to 280 nm. This range of UVR has germicidal properties.

UVC is almost totally absorbed by the stratospheric ozone layer and UVB is very absorbed (Cabrera et al., 2005).

1.2.4 Factors affecting solar radiation

One of the most frequent problems of these problems is misinformation about all the problems that come from needing to take proper care when exposed to long solar radiation. However, solar radiation is essential for many things, from producing chlorophyll in plants to obtaining vitamin D in humans thanks to sun exposure (Mendes, Hart, Lanham-new, & Botelho, 2020). It can also have severe consequences if solar radiation is high. Factors such as reducing the ozone layer have increased the ultraviolet radiation that reaches planet earth, causing skin damage and eye problems (Wang et al., 2012). Other factors such as height, clouds, solar noon, and albedo can increase the ultraviolet index, so it is recommended to be very careful when going out to open places where there is a lot of sun exposure.

Height is a factor that can contribute to UVB radiation because the higher the place, the shorter the path of UVB rays will be; likewise, the radiation absorption processes will be less (Aceituno-madera, Buendía- Eisman, Olmo, & Jiménez-Moleón, 2011). Clouds have an excellent absorption and reflection capacity, so they can absorb up to 35 to 80% of solar radiation, leaving approximately between 0% and 45% of solar radiation to reach (Garźon-Chaveza et al., 2018). Half a solar day, the intensity of solar radiation varies depending on the distance from the equator. Further away from the equator, the less the radiation intensity, while if it is closer to the equator, the greater the solar radiation and its maximum levels will arrive at noon solar day (HM Id, Hatsusaka, Shibuya, Mita, & Yamazaki, 2019). Albedo is the relationship between the irradiance that reaches the surface and the irradiance that goes out of the surface in a horizontal plane (Lester & Parisi, 2002). The value of the albedo is essential when talking about places like snow or the sea since they have an albedo with a significant value.

To finish, these factors, such as ozone, height, clouds, solar noon, and albedo, are significant since this will determine if the UVB radiation value goes up or down. At the same time, these factors can determine whether the risk of going out without protection against UVB radiation is high or low.

1.2.5 Cloud effects

According Calbó et al. (2005), the Cloud Modification Factor (CMF) depending on the type of cloud is show in Table 1.

Table 1

CMF values depending on the type of cloud.

Condition of sky	Cloud Modification Factor (CMF)
clear sky	0.992
scattered clouds	0.896
broken clouds	0.726
overcast conditions	0.316

Adapted from (Calbó et al., 2005)

But according to the cloud percentage, CMF is shown in Figure 3. Here, the figure presents the ratio between the UV with and without clouds

Figure 3

Relationship between the cloud percentage and the ratio of UV with and without clouds

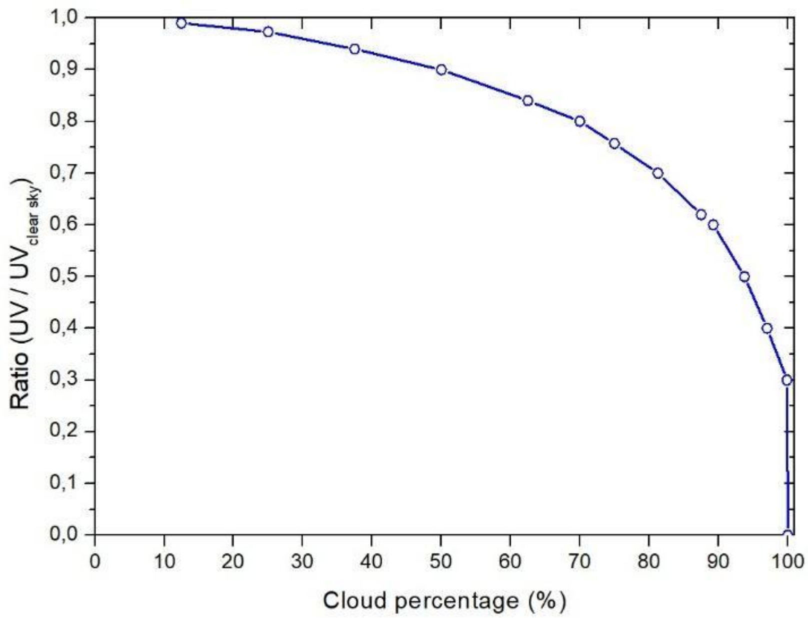

Adapted from (Calbó et al. (2005).

1.3 Models of solar radiation

1.3.1 TUV model

The TUV model is a "Tropospheric Ultraviolet-Visible Model" that calculates the spectral irradiance, photodissociation coefficients, and biological irradiances for some biological effects. This model uses a radiative transference equation based on input data such as meteorological, terrestrial, and solar parameters.

The model was implemented in Fortran 77 programming software and is open source. In particular, a rapid version (quick TUV) is available on a web page (https://www.acom.ucar.edu/Models/TUV/Interactive_TUV/). Figure 4 shows the home screen of the TUV model available on the web page.

Figure 4

Home screen of "quick TUV" available in the web page

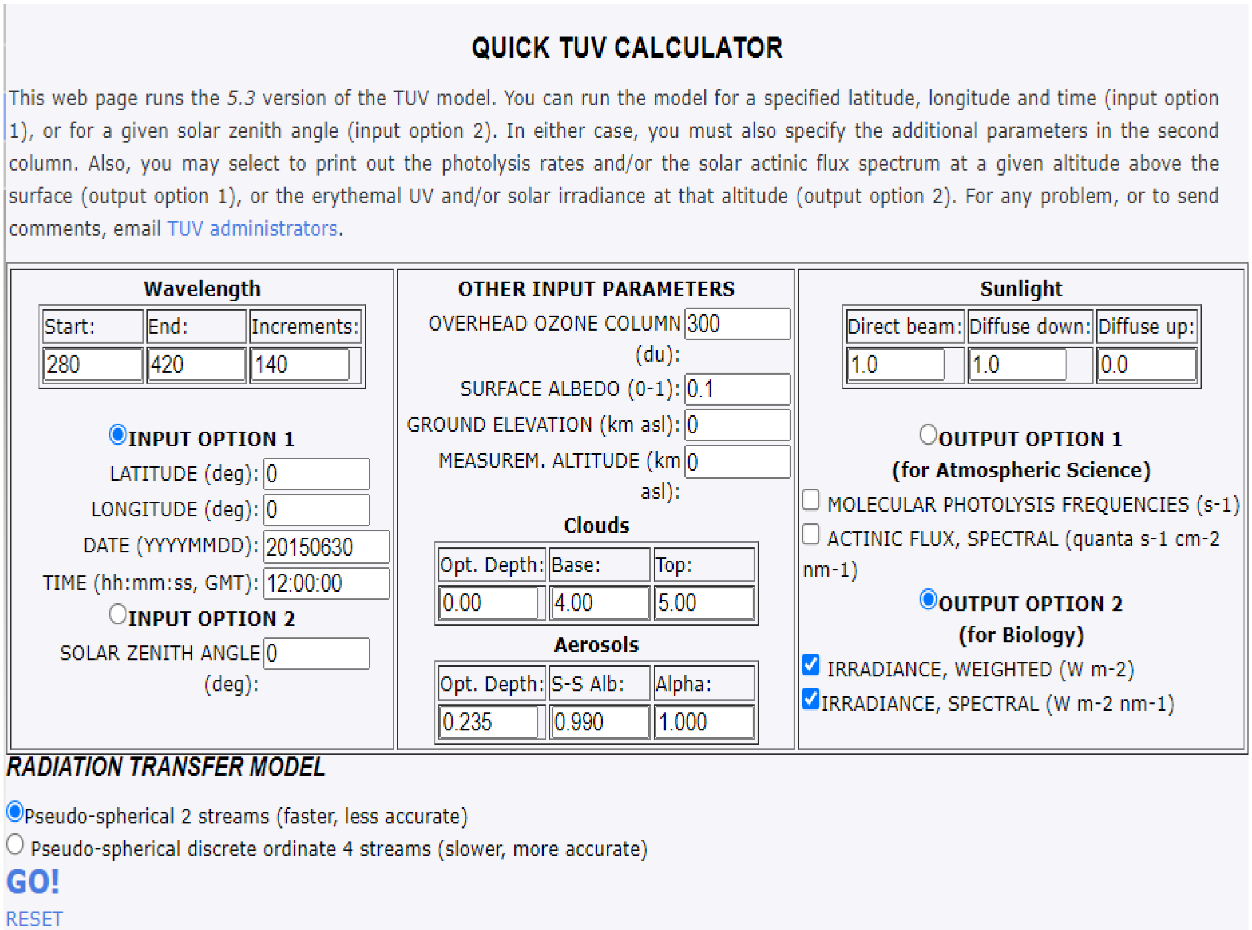

Take From (https://www.acom.ucar.edu/Models/TUV/Interactive_TUV/).

As it can be seen, the input parameters are:

- Latitude, longitude, and altitude;
- Date and time,
- Total column of ozone,
- Surface albedo,
- Ground elevation and measurement altitude,

- Optical depth of clouds and optical depth of aerosols.

This software produces two types of outputs and, in this thesis, "output option 2" was used because it provides the solar spectral irradiance and some biologically effective irradiances.

1.4 Ocular biological effects of the sun

Solar radiation from the sun has infrared, visible, and ultraviolet components. In order retina to only receive visible radiation, most harmful electromagnetic radiation must be absorbed by other structures of the eyes, and these structures can be damaged by solar radiation.

The human cornea filters the wavelength smaller than 295 nm (UVC) and is part of UVB radiation. The human lens absorbs the rest of the UVB and all the UVA. A young human lens allows a small fraction of UVB radiation (less than 320 nm) reaches the retina. Adult lenses filter the blue more than the visible radiation. Without a lens (aphakia pathology) and with blindness, there are some changes in the wavelength that reaches the retina (see Figure 5) (Cabrera et al.,).

Figure 5

Wavelength that reaches each part of the eye

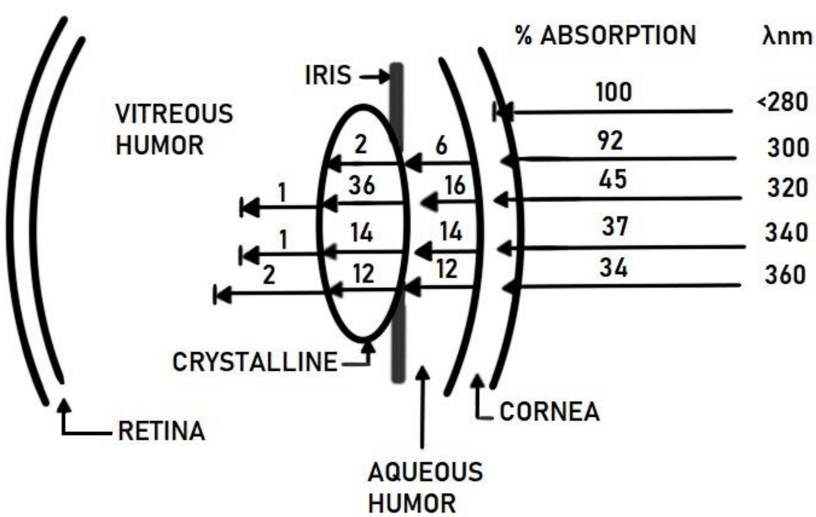

Adapted from (Cabrera et al., 2005).

1.4.1 Action spectrum

There is a handy tool to understand the wavelength more absorbed by the molecules or the wavelength of the emission peak. This tool is the *action spectrum* representing the relative effectiveness in producing the biological response of different wavelengths of light (Cashore, 2017). Therefore, the action spectrum is the way to represent the response of each tissue to each wavelength of radiation (solar or not).

There are action spectra for erythema, cataracts, photoconjunctivitis, and photokeratitis. There is no action spectrum of pterygium, but its energy received in the eye can be analyzed. When ocular pathologies are presented later, their action spectra will be presented.

It is essential to point out that, according to the bibliography, ultraviolet radiation is responsible for all mentioned effects.

1.4.2 Cataracts

Prolonged exposure to the sun without appropriate safeguards can lead to various issues, which is a widely recognized fact. Cataracts are a prevalent eye disorder caused by exposure to ultraviolet (UV) radiation, a common problem worldwide (see Fig 6) (Vaz Pereira, 2017). It is called a cataract when the lens does not allow the correct passage of light; therefore, this can lead to problems such as loss of vision (H. M. Id et al., 2019). The percentage can be reduced up to 10% using protection, just by wearing a cap or glasses to protect against the ultraviolet radiation produced by the sun (L. C. Id et al., 2021). Standard cataract treatment is removing the damaged lens and implanting an intraocular lens prosthesis. This intraocular lens can prevent the transmission of Ultraviolet light or blue light produced by electronic devices such as cell phone screens (Harada et al., 2017). The leading cause of eye diseases is prolonged ultraviolet solar radiation; therefore, great care must be taken when taking the correct measures when sunbathing since this can make the difference between losing the eye's lens and/or sight. The action spectrum of the cataract effect is shown in Figure 8-a, where the maximum effect is at 300 nm.

Figure 6

Cataract

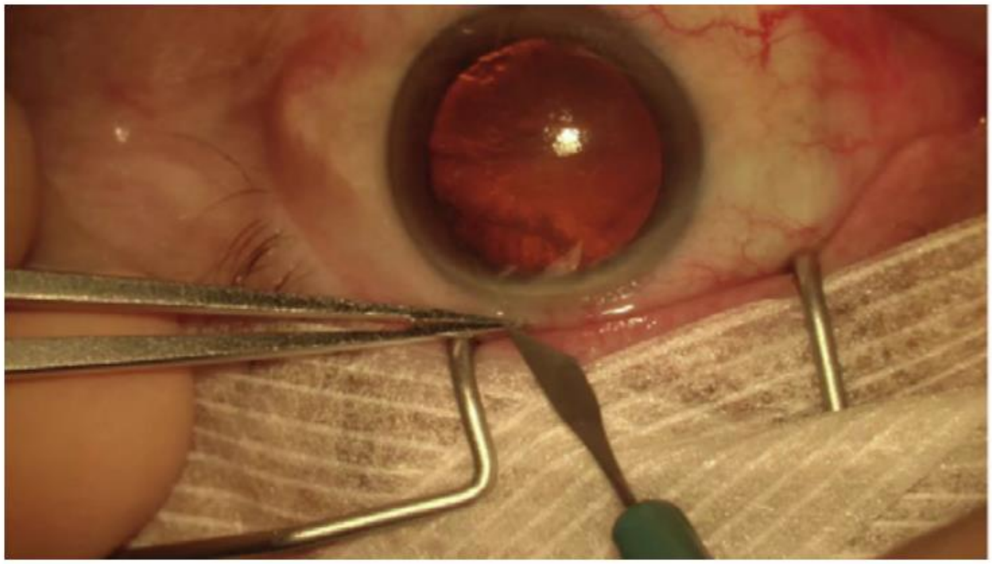

Taken from (Grammatikopoulou et al., 2021)

1.4.3 Photokeratitis

Ultraviolet radiation can cause skin burns up to skin cancer. One eye disease that causes intense patient pain is known as photokeratitis, which is also caused by exposure to ultraviolet B radiation (Chen et al., 2019). The action spectrum of the photokeratitis effect is shown in Figure 8-b, where the maximum effect is maximum at 300 nm. Photokeratitis is caused by ultraviolet b radiation, but it can also be caused by ultraviolet c radiation that comes from artificial sources such as welding machines, so it is crucial to take safety measures in the case of work such as welding, wear a helmet that prevents the entry of ultraviolet radiation c. On the other hand, photokeratitis is also known as snow blindness; this is because, at high levels of albedo, such as the level, it tends to reflect the sun's ultraviolet rays, causing damage and causing photokeratitis (Garźon-Chavez et al., 2018). One of the causes of severe pain in patients suffering from photokeratitis is due to the separation of epithelial cells (Harada et al., 2017).

For this reason, adequate protection must be taken into account in places with high solar reflection, in addition to wearing clothing and taking the necessary care at work, as this will prevent future diseases such as photokeratitis.

Figure 7

Photo of photokeratitis

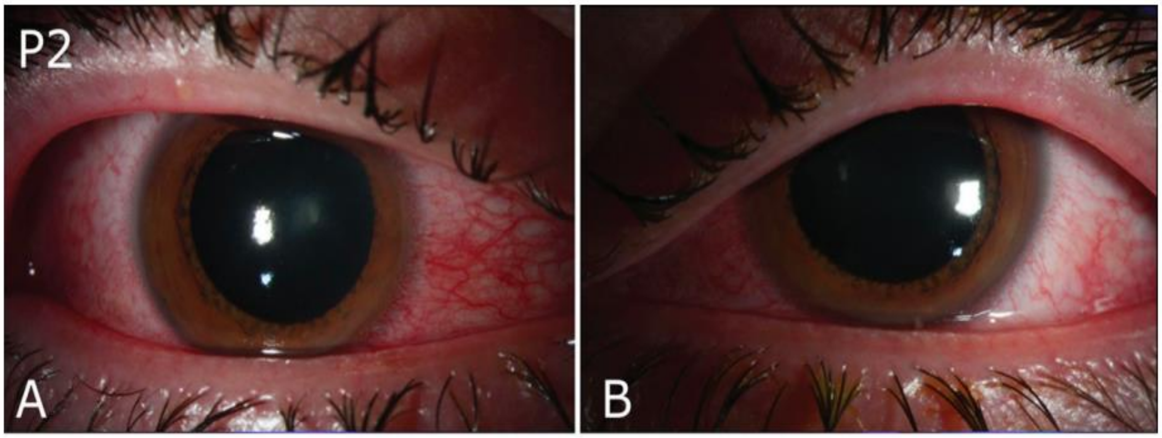

Taken from (Sengillo et al., 2020)

Figure 8

Action spectrum of ocular effects by the Sun: a- Cataracts effect; b- Photokeratitis effect, c- Photoconjunctivitis and d- Erythema effect.

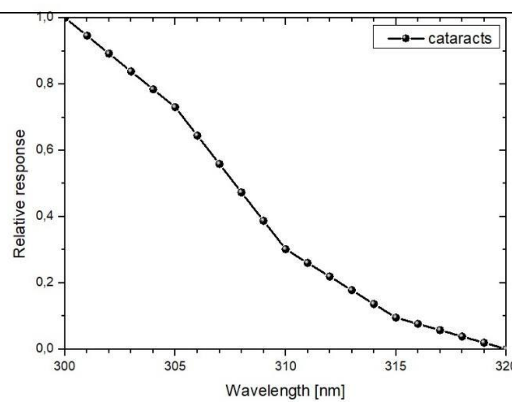

a

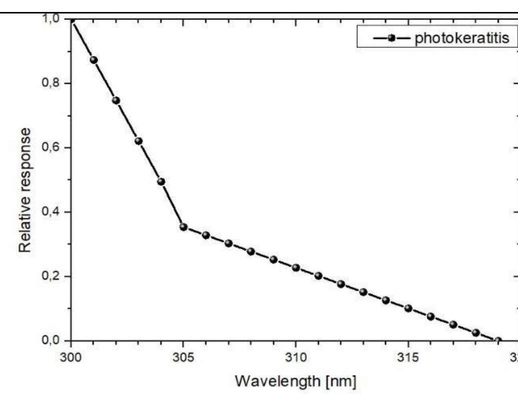

b

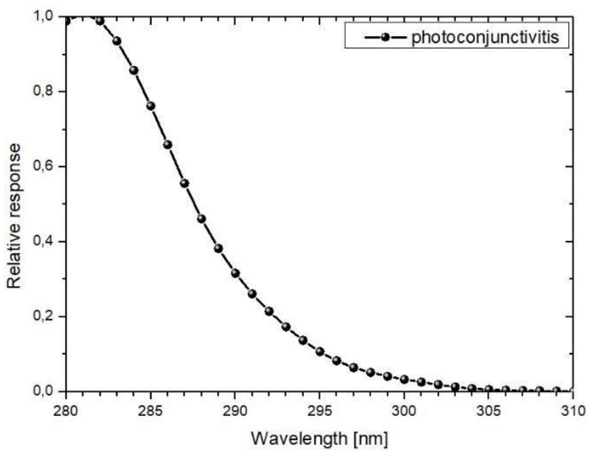

c

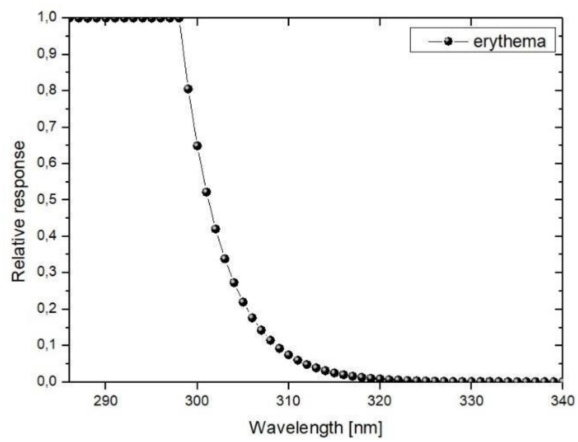

d

Adapted from (Gao et al., 2012)

1.4.4 Photoconjunctivitis

Exposure to solar radiation, specifically ultraviolet B rays, in addition to being exposed to surfaces with a high albedo index, can cause photoconjunctivitis and is often accompanied by photokeratitis. In addition to ultraviolet B rays, ultraviolet C rays from artificial sources can also cause these eye problems. Fortunately, these diseases cause little or no damage (John, Esfandiari, Loewen, & Matthew, 2021). The action spectrum of the photoconjunctivitis effect is shown in Figure 8-b, where the maximum effect is maximum at 281 nm.

1.4.5 Pterygium

Pterygium is a disease strongly related to prolonged UV exposure. It is a degeneration of the bulbar conjunctiva that has a triangular, vascularized appearance, often invading the cornea (Figure 9) (Cabrera et al., 2005; Ghoz et al., 2019).

Figure 9

Image of a pterygium

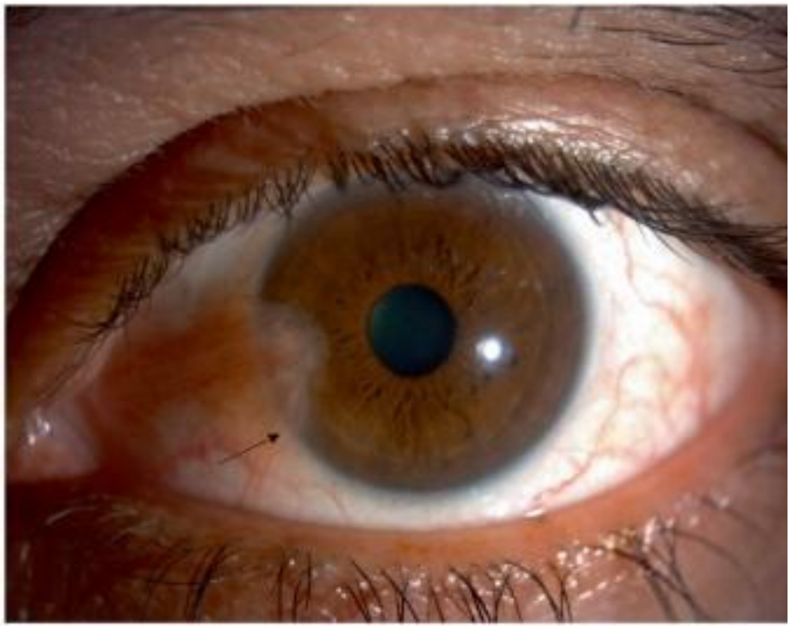

Taken from (Ghoz et al., 2019).

Pinguecula is a conjunctiva collagen degenerative process related to sun exposure. The risk of developing pterygium or pinguecula is associated with high levels of UVA and UVB. However, it was observed that the relationship between the UV radiation and the pterygium is higher than between UV and pinguecula (Cabrera et al., 2005).

The accumulative effect of UV radiation is an essential factor in developing pterygium, but there are also other factors, such as dry eyes and micro-trauma from smoke, sand, and dust particles (Cabrera et al., 2005).

Pterygium is primarily present in countries close to the equatorial zone. Therefore, countries such as Ecuador in the equatorial zone will have a higher percentage of patients with pterygium than other countries.

The progression of the pterygium occurs because solar radiation promotes the development of pro-inflammatory cytokines in addition to growth factors such as fibroblast and vascular endothelial growth factors (Wu, Xu, Sheng, Su, & Zhu, 2020).

1.4.6 Erythema

The radiation of sunlight, especially ultraviolet, is carcinogenic and has become a problem for people in general. One of the effects caused by solar radiation, apart from generating carcinogenic problems, is sunburn, better known as erythema (Matsumura & Ananthaswamy, 2004). Prolonged exposure to the sun commonly causes erythema. However, it is also known that it can be an accompaniment to a skin problem such as acne or other dermatological problem (Abdlaty & Fang, 2021). The blood vessels of the dermis cause an increase in blood on the skin's surface, which results in the reddening of the skin due to sun exposure (Photobiol, Schmalwieser, & Diffey, 2012). The action spectrum of the erythema effect is shown in Figure 8-b, where the maximum effect is at a wavelength of less than 300 nm.

Of all the action spectra of biological effects, the most popular is the erythemal action spectrum of the ICD (Commision Internationale de I'éclairage) because erythema is the most common of the effects on the population. This erythemal irradiance is obtained by integrating the weighted spectral irradiance by the CIE reference action spectrum up to 400 nm and normalized to 1 at 297 nm.

To conclude, solar radiation can cause many problems, especially ultraviolet B radiation, since it is carcinogenic. The result of reddening of the skin is the product of the accumulation of blood. Therefore, it is necessary to cover the body sufficiently to avoid burns or erythema.

Figure 10

Erythema multiforme

Taken from (Rodríguez-Pazos, Gómez-Bernal, Rodríguez-Granados, & Toribio, 2013)

1.4.7 Ultraviolet dose

It is important to note that the most important parameters, in order to determine the effect caused by a light source, are:

- emission wavelength of light source,
- emitted power of source of light,
- action spectrum of chromophore,
- exposure time.

Emitted power and exposure time will give us the value of the energy of the exposure. This energy is called *dose*, and it is a continuous subject of study and research. Some guidelines must be considered in the case of erythema and pterygium effects.

.

In the case of the erythema effect, a recommended dose is MED. MED is the Minimal Erythemal Dose that produces the erythema effect. MED depends on the skin's phototype (see table 2) (Fitzpatrick, 2009).

Table 2

Relationship between phototype of the skin and recommended MED

phototype	Burn and tan (defines the phototype)	Immediate pigment darkening	delayed tan	Constitutive color (without skin exposure)	DEM UVB (mJ/cm^2)
I.	Burns easy, never tans	No (-)	No (-)	ebony white	15-30
II.	It burns easily, they tan little with difficulty	Weak ($\pm$to +)	Minimal to weak ($\pm$to +)	White	25-40
III.	Burns moderately, tans moderately and evenly	Defined (+)	Low (+)	White	30-50
IV.	Burns little, tans moderately and easily	Moderate (+ +)	Moderate (+ +)	Beige-olive, light tan	40-60

V.	Rarely burns, tans profusely	Intense (+ + +) (brown)	Fountain, rich brown (+ + +)	Moderate brown or tan	60-90
VI.	Never burns, tans profusely	Intense (+ + +) (dark brown)	Fountain, rich brown (+ + +)	dark brown or black	90-100

Adapted from (Fitzpatrick, 2009).

2 PROBLEM STATEMENT

Around the world, about 2.2 billion people have vision deficiencies; about half of this number can prevent or have not yet entered treatment to cure these visual deficiencies. The country's economy greatly influences the number of eye diseases since a stable economy has four times fewer cases than emerging countries. Most cases of ophthalmological diseases are usually in rural areas or are of low economic resources, older adults, ethnic minorities, and indigenous populations (World Health Organization, 2019).

In Ecuador, from January to March 2021, almost half of Ecuador's population (46%) had an informal job. It was also helped by the COVID-19 pandemic, which caused the loss of formal jobs, transferring them to informal jobs (INEC, 2021). Most of these jobs do not have decent quality, and many of them are done outdoors, exposing themselves to the sun for a long time, which in the long run can lead to problems such as skin cancer or eye diseases.

Informal jobs that are usually carried out outdoors can be street vendors, farmers, bricklayers, Etc. In Ecuador, most informal workers often do not have health insurance because the job cannot provide insurance or because the workplace does not insure them. Therefore, this brings a problem since the worker who does not have health insurance will have to resort to their own money when wanting to perform a treatment (Toro & Abundiz, 2014). Paying for their treatment is often complicated since the person with these jobs does not have enough money to cover their expenses, causing discomfort for the whole family.

For this reason, it is essential to consider the days or dates on which there may be more solar radiation so as not to be exposed to eye disease or other problems such as skin cancer. In general, eye problems such as pterygium, cataracts, photokeratitis, or photoconjunctivitis can be prevented by simply wearing UVB-protective lenses or wearing a hat that covers the face from UVB radiation.

2.1 General Objective

Analyze the incidence of ultraviolet solar radiation in the generation of minor pathologies that affect and / or cause loss of vision, in the Otavalo canton of the Imbabura province

2.2 Specific Objectives

Collect data on the location, altitude, albedo, solar noon, amount of ozone, and amount of aerosol in the atmosphere in the Otavalo city for their respective studies.

Model all the data obtained to find the solar irradiance spectrum of the Otavalo city, and respective analysis will be carried out.

Develop a program with the data obtained from the irradiances, which will indicate the probability of developing an ocular pathology.

3 MATERIALS AND METHODOLOGY

The TUV model was used in order to calculate the solar biological irradiances for Otavalo city. The value of the four biological effects was calculated twice per month (the first and fifteenth days of each month) at noon in Otavalo.

Input climatological data were required to make this calculation with the TUV model. In the first analysis, the cloud content was considered null.

3.1 Satellite database

3.1.1 Google Earth

Google Earth is a tool that allows the user to obtain information on the geography of almost any point on the planet.

The Google Earth website was entered, and the program was executed to obtain the geographic data. Consequently, the desired location was sought. For this study, the Bolívar Park in the canton of Otavalo was used as a reference since it is located in the heart of the city. Therefore, the data used would be adequate for the entire city.

The data obtained from Google earth are the following: 2563m, 0'13"31'N, 78'15'50"W.

Once the data is already available, a conversion of the data from degrees, minutes, and seconds to degrees with decimals is carried out since these data will be used for later calculations in which degrees with decimals are used.

The data obtained are as follows: Latitude: 0.2252777777777778 N and Longitude: -78.26388888888889 W (see Figure 9).

Figure 11

Image of study zone.

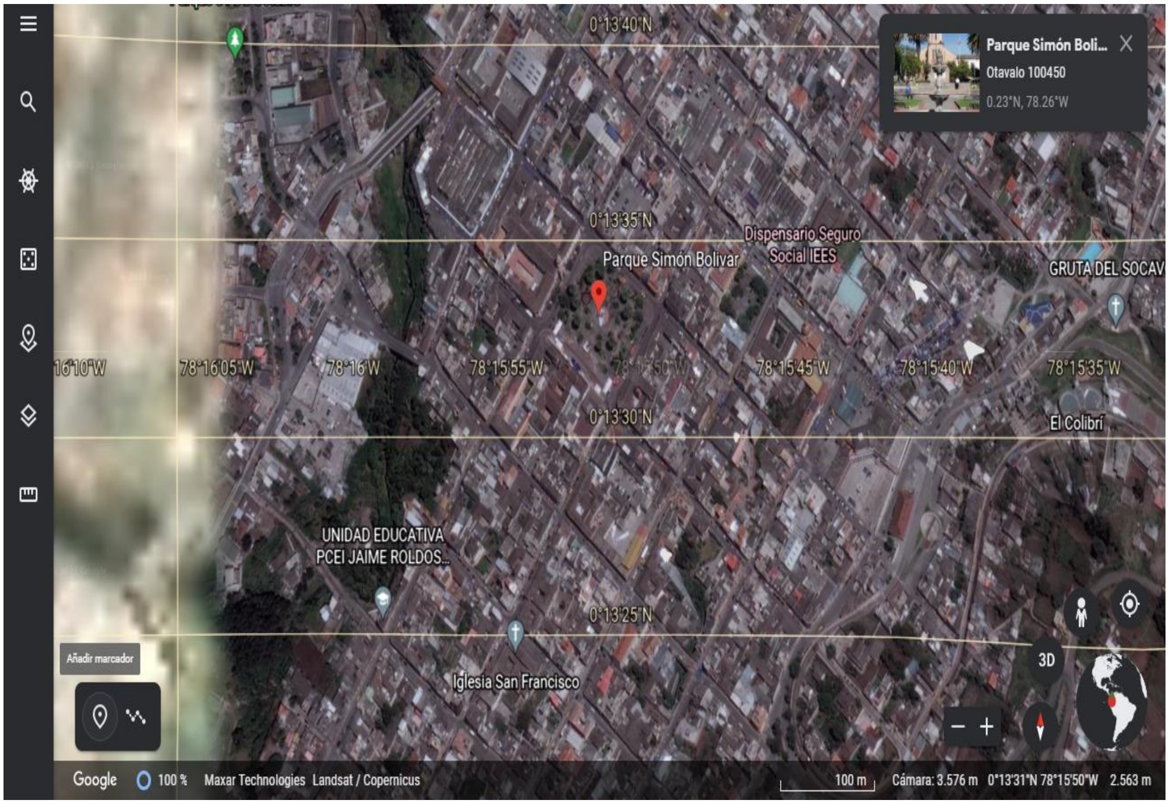

3.1.2 NOAA Solar calculator

The NOAA Solar Calculator allows the user to obtain solar noon data from anywhere in the world. Solar noon is when the sun is practically on the surface to be studied, depending on the region where the study will be carried out. NOAA Solar calculator was used to obtain the data for the solar noon:

First, go to the NOAA Solar Calculator page, where there are two parameters to fill in: location and date. The location data is filled with the data obtained with Google earth, 0.2252777777777778 N and Longitude: -78.26388888888889 W in addition to the time zone of Ecuador, which in this case is America/Guayaquil and the UTC Offset -05:00 is filled.

Then the date on which it is required to measure the solar midday is entered, which in this case will be the 1st and 15th of each month of 2010. Afterward, a table with the midday data can be extracted since the program allows obtaining the data for the whole year in a table in addition to giving sunrise and sunset data (Annex A). Finally, the same process is repeated for each year from 2010 to 2020.

3.1.3 NASA Power

NASA Power is a platform that allows obtaining solar and meteorological data worldwide. The surface albedo is the surface's reflectivity concerning solar radiation. The more albedo is on the surface, the greater the reflection of solar radiation. The albedo is much higher in places like water or snow than on sandy surfaces. To find surface albedo data:

First, the user must enter to NASA POWER (Prediction Of Worldwide Energy Resources) platform and enter the power data Access part. Next, the information necessary to access the data is entered: The community of renewable energy users is chosen. Then a temporary average is chosen between daily, monthly, annual, and climatological, for which a climatological average was used. Next, the latitude and longitude are entered with the data obtained from Google earth Latitude: 0.2252777777777778 N and Longitude: -78.26388888888889 W or there is also the option to choose the place manually. Then, the user must choose the time range from which the data is to be obtained, for which the program has preset the average data; therefore, the user will not be able to choose the range date. Next, the CSV output file format was selected. Then, the parameters of "all-sky Surface albedo" were selected to obtain the respective data.

Finally, all the required information is uploaded, and the program processes the output data. Downloaded data can be viewed in CSV format for ease of use. This data can also be downloaded in formats such as ASCII, GeoJSON, NetCDF, and NASA Power, allowing the user to download a graphic in PNG format (Annex B).

3.1.4 Deep blue aerosol optical depth

GEOVANNI NASA was used to search for aerosols, which are pollution particles. GEOVANNI NASA is a website that provides information from all over the world about precipitation, atmospheric temperature, aerosols, Etc. All this information is collected by various satellites around the world.

Once the user enters GEOVANNI NASA, there are several parameters to fill in, so the user must first look for the measurement parameter called optical depth, which is the optical depth of the aerosol, then choose a plot of an averaged time series. In the next step, the user will have to choose where he wants to obtain the data. The pixel in which the data is required to be obtained to choose the place is first defined. The pixel where the data is being recorded is one degree, and the point to be analyzed is a square of 1 degree x 1 degree. To obtain the pixel's square, subtract 0.5 degrees south, add 0.5 degrees north, and add 0.5 degrees east and 0.5 degrees west in longitude. Therefore, to obtain total ozone and Deep blue aerosol optical Depth data, degrees 79W, 0N, 78W, and 1N of the square pixel were used (Annex C).

Then the database is chosen; in this case, a daily series was used: the daily data of the optical depth at 550 nm. The database daily is Aerosol Optical Depth 550 nm (Deep Blue, Land-only). Then the date range in which the data will be given is selected. This study's data is from January 1, 2010, to December 31, 2020. Once all the information has been loaded, all data can be extracted, data can be extracted in CSV format, and a plot of data vs. dates can also be extracted in PNG format (Annex D).

3.1.5 Total column ozone

The steps to obtain the total column ozone data are similar to those used to obtain the aerosol optical depth data. The NASA web interface, also known as GEOVANNI, was used to search for the total column ozone.

First, the measurement parameter is set to total column ozone, and then an area-averaged time series plot is chosen. The next step is to choose the place where the data is going to be obtained. The exact configuration was used in the aerosol optical depth for this case. Therefore, the pixel is 1 degree x 1 degree with latitude and longitude of 79W, 0N, 78W, and 1N. In the next step, a database is searched. In this case, a database in Dobson units was used since it is the most used every time the amount of ozone in the earth's atmosphere is discussed.

In the next step, the date range to extract the data is configured, which will be from January 1, 2010, to January 31, 2020. Then the database with which to work is selected, which in this case was Time Series, Total Ozone Column (Daytime/Ascending, AIRS-only) daily. As a final step, the data is extracted in CVS format, and a graph with the data in PNG format is also extracted (Annex E).

3.2 Data interpolation

3.2.1 Aerosol optical depth

The data to be interpolated are the total ozone and the deep blue aerosol optical depth. The data interpolation was carried out with the origin program, for which the interpolation tool that the program allows to perform was used.

First, the values of the deep blue aerosol optical depth are reviewed, and there are already 4008 days of which, on certain days, the corresponding data does not exist, for which they find a value of 999999, and therefore they must be eliminated. Excel was used to eliminate the data since there is too much data, although it can be done in any other way.

Then all the aerosol optical depth data is loaded into the origin to make a graph of the aerosol optical depth data as a function of all days (Annex F). In addition, a statistic of the aerosol optical depth values was performed, and the origin was configured to show the mean value, standard deviation, and minimum and maximum data. Also, the statistics results are presented, including the average value of 0.064 and the average plus and minus the standard deviation.

3.2.2 Total Column Ozone.

For the interpolation of the total ozone data, it was done with the origin program using the interpolation tool that the program allows performing. There are approximately 4008 days, and on certain days there is no data, so to perform the total ozone interpolation, a characteristic year will be generated, that is, an average year to end the problem of the few data (Annex G). Therefore, first, the data of all January 1 between 2010 and 2020 are averaged, and so on with the other days of the year. Excel was used to perform the averages since it is a tool that allows working with several data simultaneously, but it can be done in any other way.

3.3 Procedure to calculate the biologically effective irradiance

Once the input data was obtained from satellite database, the spectral irradiances were obtained, twice per month, at solar noon with the TUV model.

Therefore, the spectral irradiances have been obtained, twice per month, these data are used to obtain the irradiation of biological effect.

When the spectral irradiance of biological effects is required, the mathematical convolution (the sum of the products for each length of wave) of the solar spectral irradiance, $I_{solar}(\lambda,t)$, with the action spectrum of the biological effect that it wants to study, $\sum(\lambda)$ must be calculated.

For example, to calculate the irradiance of cataracts ($I_{cataracts}$), then the mathematical equation to obtain $I_{cataracts}$ is shown in the equation (1).

$$I_{cataracts}(\lambda, t) = \sum_{\lambda_1}^{\lambda_2} I_{solar}(\lambda, t).\, \varepsilon_{cataracts}(\lambda) \qquad (1)$$

Now, with the $I_{cataracts}(t)$ can be obtained, in W/m^2, integrating the spectral irradiance, $I_{cataracts}(\lambda, t)$, in wavelength. The integral is a mathematical operation similar to calculate the area under the curve (equation 2).

$$I_{cataracts}(t) = \int_{\lambda_1}^{\lambda_2} I_{cataracts}(\lambda, t).\, d\lambda \qquad (2)$$

Each spectral irradiance calculation and then integrated gives only one point. In these cases, it was calculated twice per month at solar noon. These 24 irradiances are collected and graphed.

3.4 Index of biological effect of Sun over the vision

Of the four irradiances, the most commonly measured irradiance is erythema. Since this, it is important to obtain the functions to relate each of the effects' irradiances to the erythemal irradiance. This will allow the calculation of the irradiances of each effect, if the erythemal irradiance is available.

The functions that relate the studied ocular biological effects with the erythemal effect were calculated, in order to have the erythemal irradiance and determine each ocular effect.

Another point is shown in the action spectra in figure 12, it could be noted that cataracts, photokeratitis and photoconjunctivitis are strongly dependent on the UVB range and their action spectra have a similar shape to the erythematous action spectrum. This situation reinforces the fact that the UV Index is a good indicator of solar risk not only erythema but also the other effects.

Figure 12

Action spectra of different effects of UV radiation.

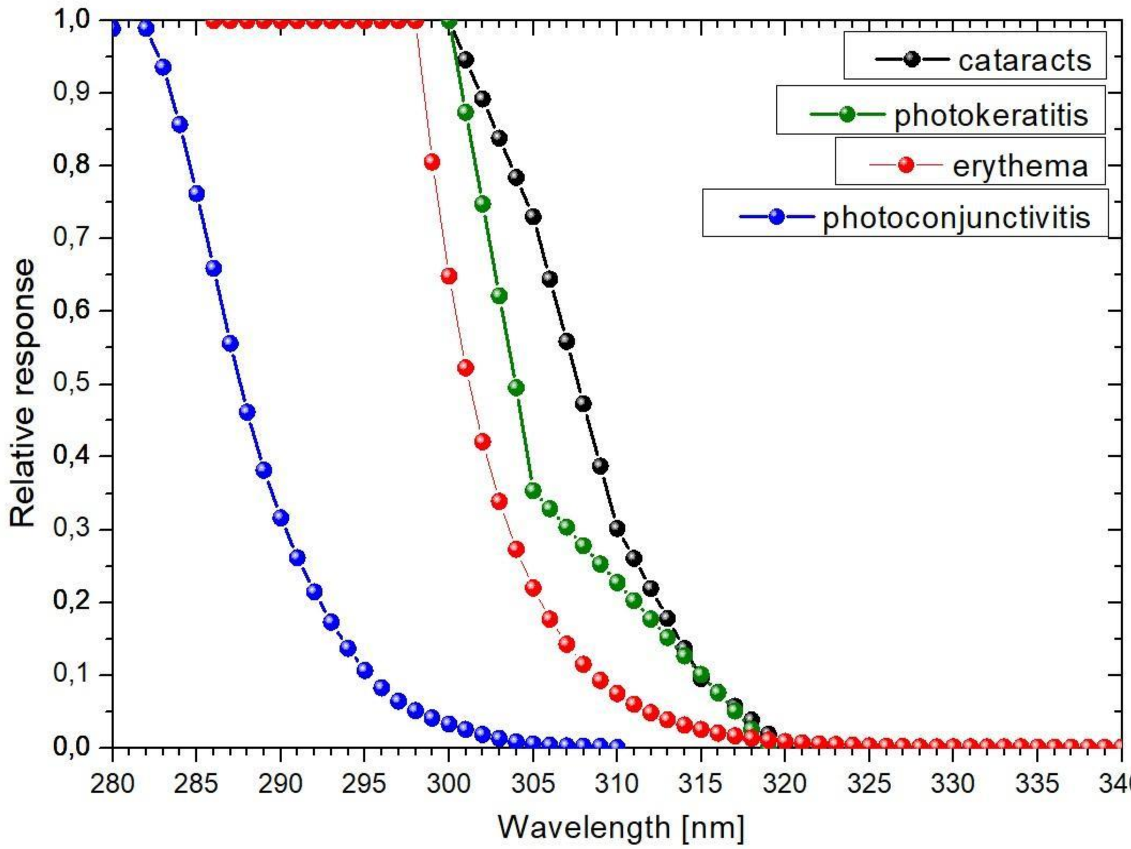

Made by me

4 RESULTS

4.1 Evolution of model input data: atmospheric components

4.1.1 Total column of ozone

Figure 13 shows the smoothed evolution of the total column of ozone whose mean value is (250.4 ± 8.4) DU, having a minimum value of 238.7 DU in January and December months and maximum value of 265.3 DU on October.

Figure 13

Annual evolution of total column of ozone fitted for Otavalo, in Dobson unit.

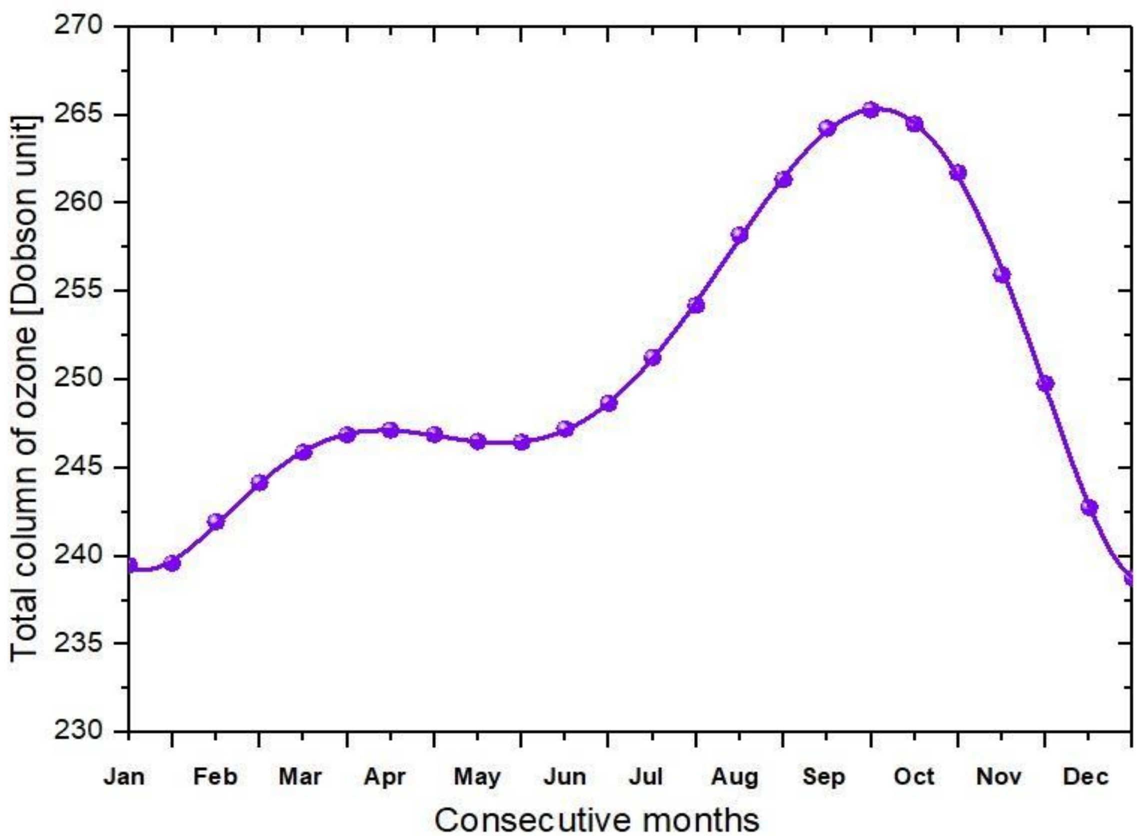

To make this figure of a characteristic year, data from 10 years was used starting from January 2010 until December 31, 2020.

4.1.2 Annual evolution of biological irradiances in Otavalo (without clouds)

Figure 14 shows the annual evolution of the biological irradiances linked to ocular pathologies such as photoconjunctivitis, cataracts and photokeratitis for Otavalo and its comparison with the erythemal irradiance.

Figure 14

Annual evolution of different biological irradiances linked to ocular pathologies (photoconjunctivitis, cataracts and photokeratitis) compared with the erythemal irradiance, at noon without clouds in Otavalo.

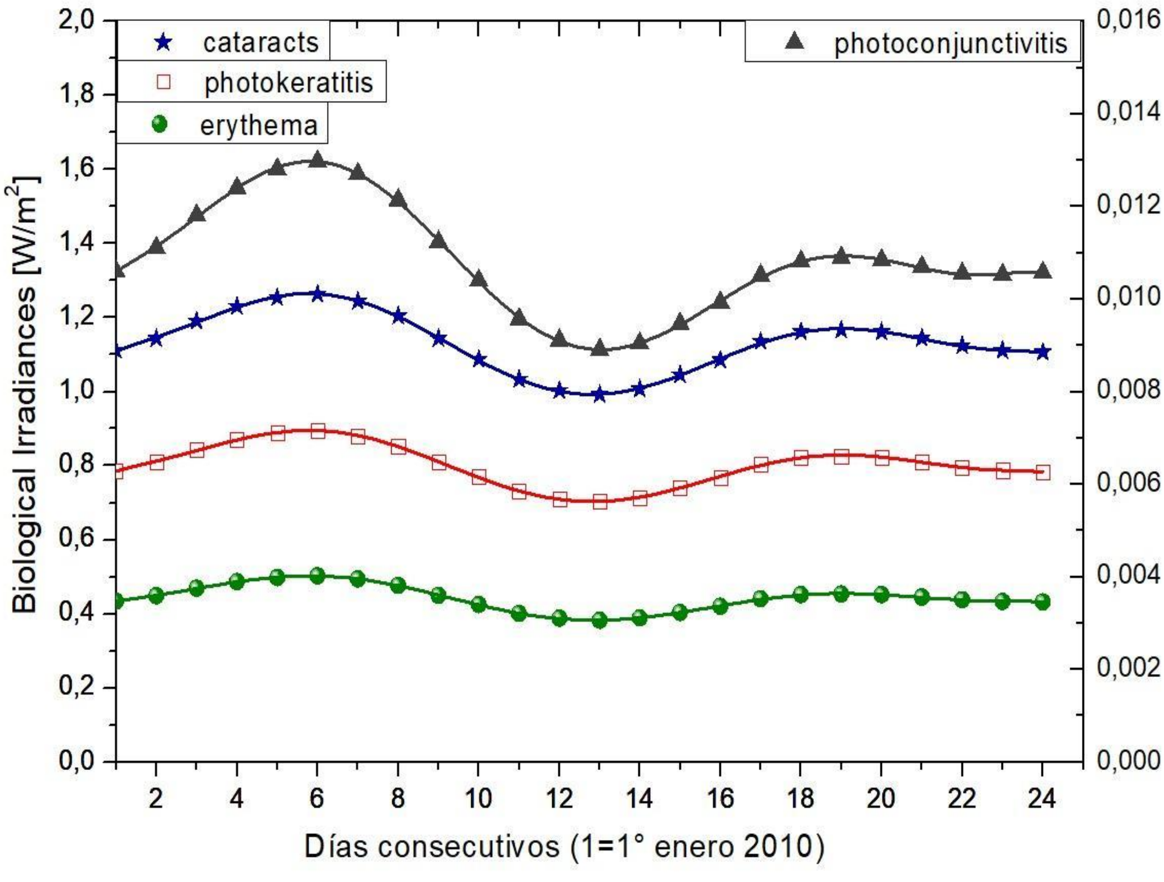

Table 3

Ranges of irradiances of different biological effects.

Irradiances [W/m^2]	Mean	Standard Deviation	Minimum	Maximum
Erythemal	0.44253	0.03443	0.38301	0.50245
Cataracts	1.13119	0.07835	0.99224	1.26334
Photokeratitis	0.80124	0.05528	0.70316	0.89442
Photoconjuncti vitis	0.01082	0.00118	0.00891	0.01297

The irradiances of different biological effects have the range of 0.01641 [W/m^2] and 0.04451 [W/m^2] in the case of erythemal, cataracts and photokeratitis. In the case of photoconjunctivitis, the range is different: from 6,83E-05 [W/m^2] to 9,59E-05 [W/m^2] (see Table 3).

In Figure 14 it is clear that the maximum and minimum values occur at the same time in all irradiances. The reason for this is the effect of air mass on different days of year.

UV Index for Otavalo has a medium value of (17.7 ± 1.38).

4.1.3 Annual evolution of biological irradiances in Otavalo (without clouds at 0 meters)

Figure 15

Annual evolution of different biological irradiances linked to ocular pathologies *(photoconjunctivitis, cataracts and photokeratitis) compared with the erythemal irradiance, at noon without clouds at 0 m.a.s.l.*

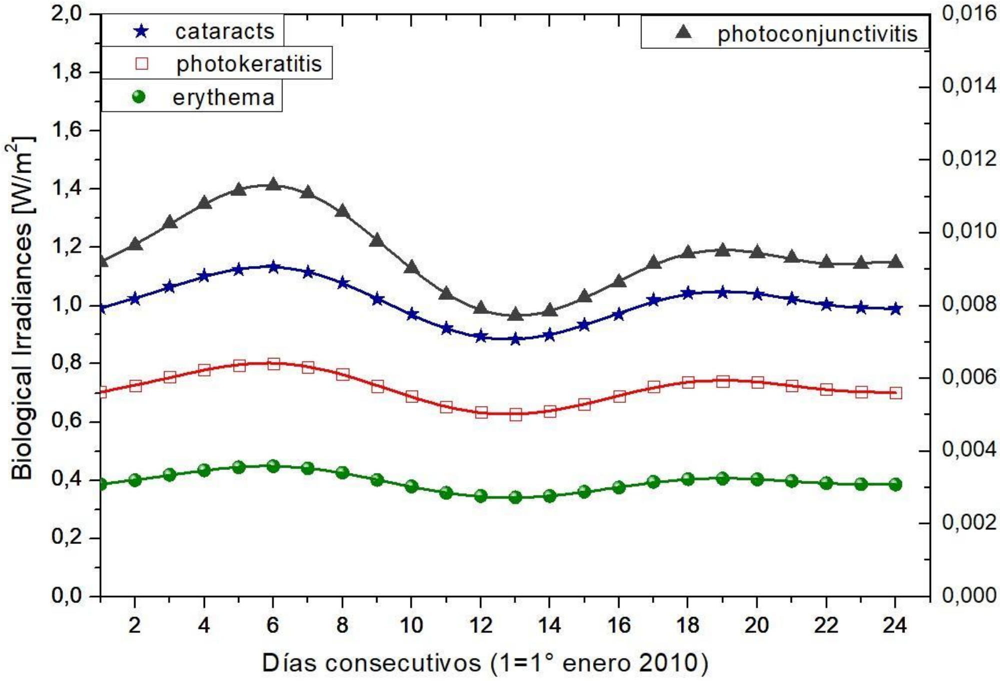

Table 4

Percentual difference between the erythemal irradiance at 0 m.a.s.l. and the erythemal irradiance in Otavalo

Irradiances [W/m^2]	Mean	Standard Deviation	Minimum	Maximum
Erythemal	0.395	0.0311	0.34073	0.44858
Cataracts	1.01181	0.0716	0.8846	1.13239

Photokeratitis	0.71708	0.05051	0.62728	0.80208
Photoconjunctivitis	9.41E-03	1.04E-03	7.73E-03	0.0113

The UVI, according Table 3, is (15.8 ± 1.24).

Comparing Table 3 with Table 4, the percentage difference between the erythemal irradiance at 0 m.a.s.l. and the erythemal irradiance in Otavalo (2563 m.a.s.l.) is:

$$Dif\% = \left(\frac{0.44253 - 0.395}{0.395}\right) \cdot 100\%$$

$$Dif\% = 12.3\%$$

Also, the difference between UVI at 0 m.a.s.l. and UVI in Otavalo (2563 m.a.s.l.) is 1.9.

4.1.4 Ocular irradiances in function of erythemal irradiance

The functions which relate each of the effects' irradiances to the erythemal irradiance are:

- FC: function that relates cataracts effect with erythemal effect;

$$I_{cataracts} = 2{,}58879 - 0{,}04748 \cdot I_{erit}^{1} + 0{,}02381 \cdot I_{erit}^{2} - 0{,}0076 \cdot I_{erit}^{3} + 0{,}00129 \cdot I_{erit}^{4} - 1{,}16886 \cdot 10^{-4} \cdot I_{erit}^{5} + 5{,}72012 \cdot 10^{-6} \cdot I_{erit}^{6} - 1{,}4353 \cdot 10^{-7} \cdot I_{erit}^{7} + 1{,}44998 \cdot 10^{-9} \cdot I_{erit}^{8}$$

- FPK: function that relates photokeratitis with erythemal effect;

$$I_{photoker} = 1{,}83334 - 0{,}03312 \cdot I_{erit}^{1} 0{,}01668 \cdot I_{erit}^{2} - 0{,}00539 \cdot I_{erit}^{3} + 9{,}242 \cdot 10^{-4} \cdot I_{erit}^{4} - 8{,}39152 \cdot 10^{-5} \cdot I_{erit}^{5} + 4{,}11459 \cdot 10^{-6} \cdot I_{erit}^{6} - 1{,}03341 \cdot 10^{-7} \cdot I_{erit}^{7} + 1{,}04438 \cdot 10^{-9} \cdot I_{erit}^{8}$$

- FPC: function that relates photoconjunctivitis with erythemal effect.

$$I_{photoconj} = 0{,}02328 + 0{,}00167 \cdot I_{erit}^{1} - 8{,}44472 \cdot 10^{-4} \cdot I_{erit}^{2} + 2{,}67176 \cdot 10^{-4} \cdot I_{erit}^{3} - 4{,}50596 \cdot 10^{-5} \cdot I_{erit}^{4} + 4{,}05555 \cdot 10^{-6} \cdot I_{erit}^{5} - 1{,}97829 \cdot 10^{-7} \cdot I_{erit}^{6} + 4{,}95209 \cdot 10^{-9} \cdot I_{erit}^{7} - 4{,}9931 \cdot 10^{-11} \cdot I_{erit}^{8}$$

4.1.5 Annual evolution of biological irradiances in Otavalo (with clouds)

In figure 16, it is shown to see the changes of UV Index with different cloudiness. This calculation was made considering the results of Figure 14 of this thesis.

Figure 16

Values of UV Index with percentage of clouds (0, 25, 50, 75 and 100%).

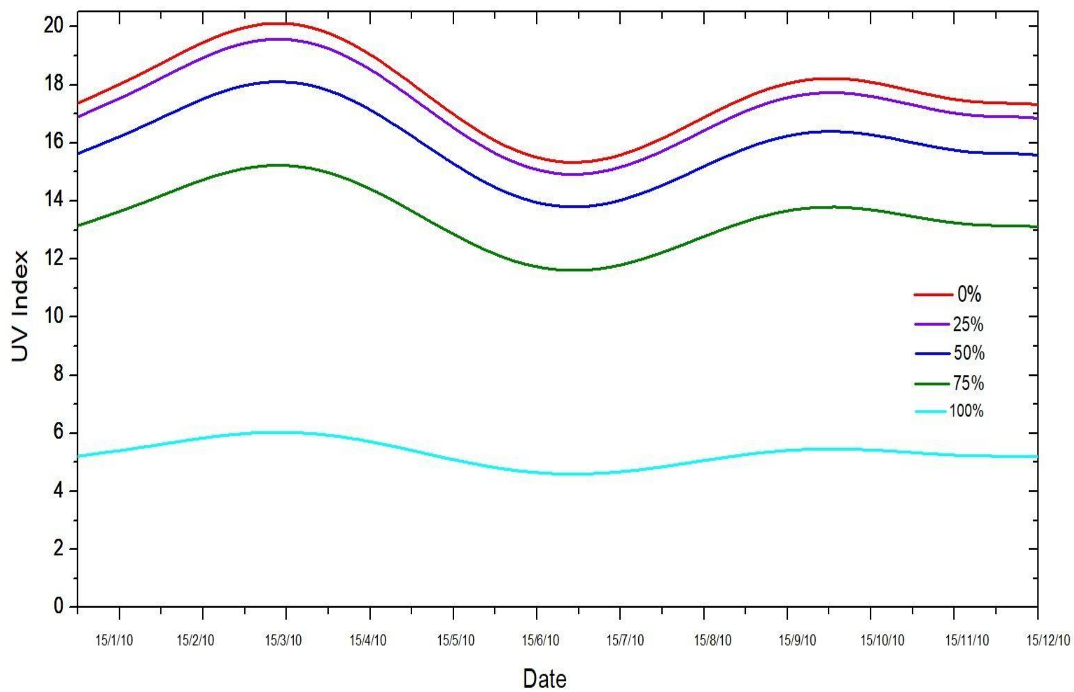

4.1.6 Index of ocular solar risk

In function of the previous results, in order to have an Index of ocular, it was proposed to use the UV Index of solar risk linked with the skin effect of the Sun.

In order to show this information to the public, a software was developed.

The data obtained were represented by graphics produced by a program, which shades the Otavalo area on the map of Ecuador with different colors depending on its irradiation.

The program was implemented with the Python version 3.9 programming language and libraries were necessary for image processing such as open-cv and others that provide mathematical functions such as numpy. Furthermore, the data was inserted into a txt file to be used as input parameters.

The main functions are described as follows:

Read the image. OpenCv provides a function called *cv2.read()* which reads the image.

Open and read the txt file. The functions *with open()* y *readlines()* allow to open and read all lines of a file where each element is a line in the file. It is also necessary to use the functions *strip()* y *split()* to remove whitespace and separate elements by a ´, ´.Shading.

Show the image. To draw the rectangle, the function was used *cv2.rectangles()* of openCV, which uses as input parameters the position of the rectangle, the color and the thickness. In addition, ranges were established to define the color of the rectangle.

Shading. The shading of the rectangle was achieved by mixing the original image with a white mask of the same dimensions to draw the figure. For this, functions such as *shapes=np.zeros_like()*, that creates the mask and *cv2.addWeighted()* which mixes and creates the shading.

Show the image. Use openCV functions like *cv2.imwrite() which saves the new image to a new file and cv2.imshow ()* which displays the image output on the screen.

The resulting image is obtained by inserting the date in the format *‘dd-mm’*.

For a better understanding of the algorithm, a flowchart has been created where it shows how the algorithm works, as can be seen in Figure 17.

Figure 17

program flowchart

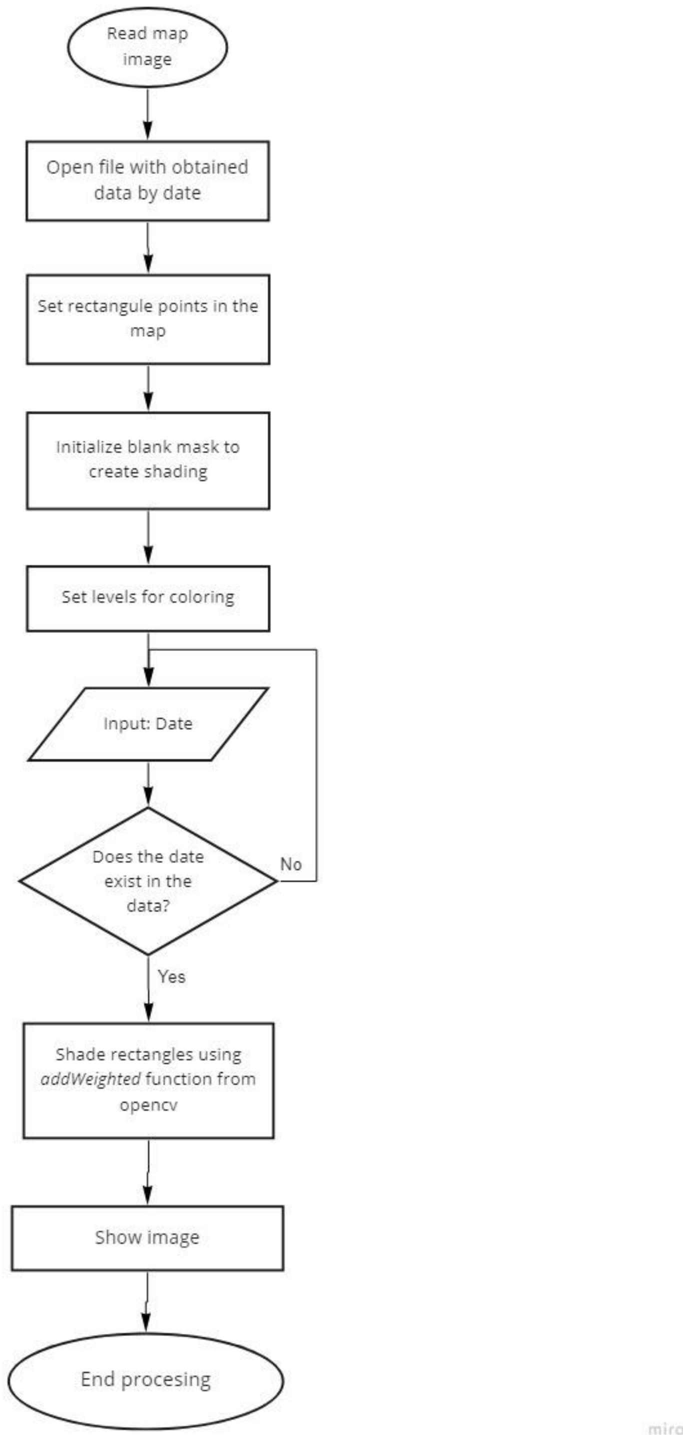

5 ANALYSIS AND DISCUSSION

The results are divided by the number of days and classified into four groups: low, medium, high and extreme, according to the ultraviolet index:

For the days from 144 to 255 and from 331 to 365, the months of June, July, August and the end of December, solar radiation is low so that people can carry out all their activities without running any risk; the UV index on those days is the lowest of all.

Between the days from 1 to 37, from 129 to 143 and from 256 to 330, the months of January to the beginning of February, mid-May, and mid-September to November are the months of the year with a medium-level UV index. The UV index so there is not much risk of an eye injury.

On days 38 to 59 and from 114 to 128, which are more or less the month of February, and between April and May, the ultraviolet index will be high. The UV index is higher than usual, so there is a risk of eye injury.

On the days between 60 and 113, more or less in March and April, the UV index is very high. The UV index is the highest compared to the other days of the year, and there is a high risk of an eye injury.

On the other hand, comparing it with a study carried out in Arica, Chile, specific differences can be noted, such as the dates of the high ultraviolet index in Otavalo, in March and April, while, in Arica, Chile, they are in the months between January and February. Likewise, during January and February, the level of the ozone layer is deficient, which is why it reacts to the increase in ultraviolet radiation (Rivas & Rojas, 2018). In Otavalo, ozone layer levels are low in March and April, fulfilling this relationship between lower ozone layer levels and higher ultraviolet radiation.

In other studies of future projections of solar radiation considering the ozone layer for the tropics, simulations with CCM (chemical-climatic model) were carried out. In 3 different GHG (greenhouse gas) scenarios with different RCP (representative concentration path) of 4.5, 6 and 8.5. The projection of the RCP of 6.0 resulted in specific regions, such as the South American region showing results such that, by the end of the 21st century, solar radiation will increase by up to 15%, mainly due to the ozone layer will decrease (Bais et al., 2019).

In conclusion, it can be seen that another study carried out in Chile has a pattern similar to that obtained by the results of this work, in addition to a study that shows that the future projection of solar radiation can increase by up to 15% more at the end of the year. of the 21st century. These data obtained should be taken into account to exercise caution in the use of protection for both eyes and body.

6 CONCLUSION

The eye problems that affect many people in the world can be caused by ultraviolet radiation, but primarily by ultraviolet B radiation, the latter being the cause of many diseases such as pterygium, cataracts, photokeratitis and photoconjunctivitis.

Some diseases, such as photokeratitis or photoconjunctivitis, can be caused by being exposed to a high intensity of solar radiation. Other diseases, such as pterygium or cataracts, can be the product of being exposed for many days to prolonged exposure to solar radiation, but most of these diseases can be prevented by taking adequate precautions against ultraviolet radiation, such as a hat or glasses sun with UVB protection. However, if the person has any of these diseases and is not treated correctly, it can lead to much more severe problems, such as loss of vision.

The latitude, longitude and altitude data of the respective place where the study was carried out were collected, in addition to other data that affect solar radiation, such as solar noon, albedo, aerosol optical depth and total column ozone. Then the data obtained from the city of Otavalo were analyzed. Then the TUV model was used, filling in all the respective parameters, and the incidence of UV radiation in the generation of ocular pathologies was observed.

Eye diseases are closely related to places with a lot of UV radiation. UV radiation can affect more or less depending on whether or not certain factors are met, such as height, clouds, ozone, aerosol optical depth, and albedo. In the case of height, it was observed that there is a directly proportional relationship since the higher the altitude, the greater the solar radiation. The same happens in the case of the albedo since it was observed that the higher the albedo, the greater the reflection of ultraviolet rays. However, in the case of clouds, an inversely proportional relationship was observed since the greater the number of clouds in the area, the lower the UV radiation index. The same occurs with ozone since the higher the ozone level, the lower the UV radiation.

On the other hand, the data obtained for June, July, August and December show that UV radiation levels tend to be low compared to the other months. the person can go out with peace of mind to do any outdoor activity.

Although, there is a relatively normal level of ultraviolet radiation for January, the beginning of February, mid-May, and mid-September to November. However, it is recommended to continue wearing protection such as glasses or a cap as an added precaution to avoid any eye injury.

In the data obtained from the study, it can be seen that the UV index is high for February and the last days of April and the first week of May. Therefore, it is marked as dangerous, and if the person wishes to go outdoors, it is recommended to use sunscreen since, these days, care must be taken when carrying out activities or going to work.

Throughout March and most of April, it was possible to observe that the radiation levels were the highest in the entire study, so great care must be taken. It is recommended not to leave the house as much as possible, but Anyone who wants to do any outdoor activity during those days should take due precautions as they may suffer from eye disease or a burn on their body.

The data obtained from ozone and UV radiation showed a relationship between the days with the highest ultraviolet index and the days with the lowest ozone concentration.

In order to facilitate obtaining the data, a Python program was developed that can display the ultraviolet index with different colors depending on the level of ultraviolet UV radiation. The colors used are yellow, representing a low UV index; orange, representing a medium UV index; red, representing a high UV index; purple, indicating an extreme UV index.

In conclusion, solar radiation is vital for humans, but exposure without proper protection can cause many problems, including eye problems. Protection such as wearing a hat or glasses to protect against ultraviolet radiation should be considered.

7 RECOMMENDATION

To search for data in GEOVANNI NASA, it is recommended that, when filling in the location data, that is, the pixel that is going to be used is equal to the pixel that the different databases have since specific databases do not have pixels smaller than those are compatible with the location pixel settings and will end up throwing an error.

When searching for the aerosol optical depth in the GEOVANNI database, it is recommended to use a database that uses data at 550nm for greater ease when performing the following data calculations in the TUV model.

For the extraction of GEOVANNI data, it is recommended to download them in CSV format for greater ease of use.

To search for the total ozone column, it is recommended to use a database that uses Dobson measurements for greater ease when performing the following calculations in the TUV model.

To make the interpolation of the optical Depth aerosol data, it is recommended to delete the data that has the number 99999999 since these are data that have no value, for which these data must be deleted because trying to continue without deleting this data could confuse when viewing the results.

8 REFERENCES

Abdlaty, R., & Fang, Q. (2021). Skin Erythema Assessment Techniques. *Clinics in Dermatology*. https://doi.org/10.1016/j.clindermatol.2021.03.006

Aceituno-madera, P., Buendía-eisman, A., Olmo, F. J., & Jiménez-moleón, J. J. (2011). *Melanoma , altitud y radiación UVB*. *102*(3). https://doi.org/10.1016/j.ad.2010.08.003

Augusto, C., & Jorge, D. (2015). *Mecanismo de fototraducción de la melanopsina en las células ganglionares retinianas intrínsecamente fotosensibles (ipRGC)*.

Bais, A. F., Bernhard, G., Mckenzie, R. L., Aucamp, P. J., Young, P. J., Ilyas, M., … Deushi, M. (2019). *Ozone–climate interactions and effects on solar ultraviolet radiation*. https://doi.org/10.1039/c8pp90059k

Benson, N. C., Manning, J. R., & Brainard, D. H. (2014). *Unsupervised Learning of Cone Spectral Classes from Natural Images*. *10*(6). https://doi.org/10.1371/journal.pcbi.1003652

Blumthaler, Ambach, and Ellinger, 1997. Increase in solar UV radiation with altitude. Journal of Photochemistry and Photobiology B: Biology, 39, 130-134.

Bony, S., Stevens, B., Frierson, D. M. W., Jakob, C., Kageyama, M., Pincus, R., … Sobel, A. H. (2015). Clouds , circulation and climate sensitivity. *Nature Publishing Group*, *8*(4), 261–268. https://doi.org/10.1038/ngeo2398

Brainard, D. H. (2015). *Color and the Cone Mosaic*. https://doi.org/10.1146/annurev-vision-082114-035341

Cabrera S, Lissi E and Honeyman J (editors), 2005. Radiación ultravioleta y salud. Editorial Universitaria. Santiago de Chile, Chile.

Calbó J., Page D. and González J.A., 2005. Empirical studies of cloud effects on UV radiation: a review. Reviews of Geophysics, 43.

Cashore W.J., Chapter 96: "Neonatal bilirubin metabolism", pp:929, in: Fetal and Neonatal Physiology. Vol. 1. Fifth Edition, ISBN: 978-0-323-35214-7, 2017

Chen, S., Lee, C., Lin, T., Peng, H., Liu, H., Chen, Y., & Tseng, K. (2019). *Protective Effects of Fucoxanthin on Ultraviolet B-Induced Corneal Denervation and Inflammatory Pain in a Rat Model*. 1–14. https://doi.org/10.3390/md17030152

Cholewiak, S. A., & Banks, M. S. (2019). *Contributions of foveal and non-foveal retina to the human eye ' s focusing response Vivek Labhishetty*. *19*, 1–15.

Gao, N., Hu, L., Gao, Q., Ge, T., Wang, F., Chu, C., … Liu, Y. (2012). *Diurnal Variation of Ocular Exposure to Solar Ultraviolet Radiation Based on Data from a Manikin Head*. (23), 736–743. https://doi.org/10.1111/j.1751-1097.2012.01094.x

Garźon-Chaveza, D. R., Quentind, E., Harrison, S. L., Parisi, A. V., Butler, H. J., & Down, N. J. (2018). *The geospatial relationship of pterygium and senile cataract to ambient solar ultraviolet in tropical Ecuador*. https://doi.org/10.1039/C8PP00023A

Ghoz N., Britton J., Ross A.R., Mohammed I. Hogan E., Said D.G. and Dua H.S., 2019. Management of primary pterygium with intra-lesional injection of 5 flurouracil and bevacizumab. Eye, 33:1776–1783 – DOI: 10.1038/s41433-019-0493-0

Grammatikopoulou, M., Flouty, E., Kadkhodamohammadi, A., Quellec, G., Chow, A., Nehme, J., … Stoyanov, D. (2021). CaDIS : Cataract dataset for surgical RGB-image segmentation. *Medical Image Analysis*, *71*, 102053. https://doi.org/10.1016/j.media.2021.102053

Harada, F., Morikawa, T., Lennikov, A., Mukwaya, A., Schaupper, M., Uehara, O., … Lagali, N. (2017). *Protective Effects of Oral Astaxanthin Nanopowder against Ultraviolet-Induced Photokeratitis in Mice*. *2017*.

Id, H. M., Hatsusaka, N., Shibuya, E., Mita, N., & Yamazaki, M. (2019). *Association between ultraviolet radiation exposure dose and cataract in Han people living in China and Taiwan : A cross-sectional study*. 1–14. https://doi.org/10.6084/m9.figshare.7992206

Id, L. C., Chang, Y., Shieh, C., Yu, J., & Yang, M. (2021). *Relationship between practices of eye protection against solar ultraviolet radiation and cataract in a rural area*. 1–12. https://doi.org/10.1371/journal.pone.0255136

INEC. (2021). *Mercado Laboral Trimestre enero-marzo*.

Jaadane, I., Boulenguez, P., Carré, S., Savoldelli, M., Martinsons, C., & Torriglia, A. (2015).

Retinal damage induced by commercial Light Emitting Diodes (LED). *Free Radical Biology and Medicine*. https://doi.org/10.1016/j.freeradbiomed.2015.03.034

John, E., Esfandiari, H., Loewen, N. A., & Matthew, R. (2021). *Association between conventional or blue-light- filtering intraocular lenses and survival in bilateral cataract surgery patients*.

Karam, H. A., & Rojas, J. L. F. (2017). *Ultraviolet solar radiation in the tropical central Andes (12.0°S)*. (November 2013), 954–971. https://doi.org/10.1039/c6pp00161k

Kels, B. D., Grzybowski, A., & Grant-kels, J. M. (2015). Human ocular anatomy. *Clinics in Dermatology*, *33*(2), 140–146. https://doi.org/10.1016/j.clindermatol.2014.10.006

Lamb, T. D. (2016). *Why rods and cones ?* (October 2015), 179–185. https://doi.org/10.1038/eye.2015.236

Lester, R. A., & Parisi, A. V. (2002). *Spectral ultraviolet albedo of roofing surfaces and human facial exposure*. *81*, 75–81.

Matsumura, Y., & Ananthaswamy, H. N. (2004). *Toxic effects of ultraviolet radiation on the skin*. *195*, 298–308. https://doi.org/10.1016/j.taap.2003.08.019

Mcneill, K. (2019). *Environmental Science Processes & Impacts Updated and validated solar irradiance reference photodegradation rates †*. https://doi.org/10.1039/c8em00478a

Mendes, M. M., Hart, K. H., Lanham-new, S. A., & Botelho, B. (2020). *Exploring the Impact of Individual UVB Radiation Levels on Serum 25-Hydroxyvitamin D in Women Living in High Versus Low Latitudes : A Cross-Sectional Analysis from the D-SOL Study*.

Organizacion Mundial de la Salud. (2019, Octubre 8). *La OMS presenta el primer Informe mundial sobre la visión*. Retrieved from Organizacion Mundial de la Salud: https://www.who.int/es/news/item/08-10-2019-who-launches-first-world-report-on-vision

PennState CEMS web page - PennState College of Earth and Mineral Sciences web page - Chapter 6.4 The Solar Spectrum - https://www.e-education.psu.edu/meteo300/node/683

Photobiol, P., Schmalwieser, A. W., & Diffey, B. (2012). *A library of action spectra for erythema and pigmentation*. 251–268. https://doi.org/10.1039/c1pp05271c

Rivas, M., & Rojas, E. (2018). *Effects of ozone layer variation in Ultraviolet solar radiation level received at ground in Arica north of Chile Effects of ozone layer variation in Ultraviolet solar radiation level received at ground in Arica north of Chile*.

Rodríguez-Pazos, L., Gómez-Bernal, S., Rodríguez-Granados, M. T., & Toribio, J. (2013). Photodistributed Erythema Multiforme. *Actas Dermo-Sifiliográficas (English Edition)*, *104*(8), 645–653. https://doi.org/10.1016/j.adengl.2012.01.024

Sabesan, R., Schmidt, B. P., Tuten, W. S., & Roorda, A. (2016). *The elementary representation of spatial and color vision in the human retina*. (September).

Sengillo, J. D., Kunkler, A. L., Medert, C., Fowler, B., Shoji, M., Pirakitikulr, N., … Uv-photokeratitis, G. A. (2020). UV-Photokeratitis Associated with Germicidal Lamps Purchased during the COVID-19 Pandemic UV-Photokeratitis Associated with Germicidal Lamps Purchased during the COVID-19 ABSTRACT. *Ocular Immunology and Inflammation*, *00*(00), 1–5. https://doi.org/10.1080/09273948.2020.1834587

Tkachev, S. Y., Mitrin, B. I., Karnaukhov, N. S., Sadyrin, E. V, Voloshin, M. V, Maksimov, A. Y., … Tkacheva, M. S. (2020). Visualization of different anatomical parts of the enucleated human eye using X-ray micro-CT imaging. *Experimental Eye Research*, 108394. https://doi.org/10.1016/j.exer.2020.108394

Toro, J. T., & Abundiz, S. V. (2014). *MARCO LEGAL E INSTITUCIONAL*. 101–110.

Vaz Pereira, S. (2017). RETINAL LIGHT EXPOSURE A F T E R C ATA R A C T S U R G E R Y ,. *Points de Vue – International Review of Ophthalmic Optics*, (February), 1–6.

Wang, F., Gao, Q., Hu, L., Gao, N., Ge, T., Yu, J., & Liu, Y. (2012). *Risk of Eye Damage from the Wavelength-Dependent Biologically Effective UVB Spectrum Irradiances*. *7*(12), 1–8. https://doi.org/10.1371/journal.pone.0052259

Wang, Y., & Chodosh, J. (2019). *Angiography of the Limbus and Cornea*. *59*(4), 19–29.

Wu, S. Q., Xu, Q. I. B. I. N., Sheng, W. E. N. Y. A. N., Su, L. I. N. Y. A., & Zhu, L. I. W. E. I. (2020). *A novel role for Livin in the response to ultraviolet B radiation and pterygium development*. 1103–1111. https://doi.org/10.3892/ijmm.2020.4481

9 ANNEXES

Annex A

NOAA Global Monitoring Laboratory
Global Radiation Group
https://gml.noaa.gov/grad/solcalc

Solar Noon Table for 2010

Location: Latitude 0.22528 Longitude -78.26389

Time Zone Offset: America/Guayaquil -5.0

All times are in local time. Cells with light green color indicate when daylight savings time is in effect.

Day	Jan	Feb	Mar	Apr	May	Jun	Jul	Aug	Sep	Oct	Nov	Dec
1	12:16:42	12:26:41	12:25:22	12:16:52	12:10:08	12:10:54	12:16:56	12:19:23	12:13:01	12:02:42	11:56:36	12:02:09
2	12:17:10	12:26:48	12:25:10	12:16:34	12:10:01	12:11:04	12:17:08	12:19:18	12:12:42	12:02:22	11:56:35	12:02:32
3	12:17:38	12:26:55	12:24:57	12:16:17	12:09:55	12:11:14	12:17:19	12:19:14	12:12:23	12:02:03	11:56:35	12:02:55
4	12:18:05	12:27:01	12:24:44	12:15:59	12:09:49	12:11:24	12:17:30	12:19:08	12:12:03	12:01:45	11:56:35	12:03:20
5	12:18:32	12:27:06	12:24:31	12:15:42	12:09:44	12:11:34	12:17:40	12:19:02	12:11:43	12:01:27	11:56:37	12:03:44
6	12:18:59	12:27:10	12:24:17	12:15:25	12:09:40	12:11:45	12:17:50	12:18:56	12:11:23	12:01:09	11:56:39	12:04:10
7	12:19:24	12:27:13	12:24:02	12:15:08	12:09:36	12:11:56	12:18:00	12:18:49	12:11:03	12:00:51	11:56:42	12:04:35
8	12:19:50	12:27:16	12:23:48	12:14:52	12:09:32	12:12:08	12:18:09	12:18:41	12:10:42	12:00:34	11:56:46	12:05:02
9	12:20:15	12:27:18	12:23:33	12:14:35	12:09:29	12:12:19	12:18:18	12:18:32	12:10:21	12:00:17	11:56:51	12:05:28
10	12:20:39	12:27:19	12:23:17	12:14:19	12:09:27	12:12:31	12:18:27	12:18:24	12:10:01	12:00:01	11:56:57	12:05:55
11	12:21:03	12:27:19	12:23:01	12:14:03	12:09:25	12:12:44	12:18:35	12:18:14	12:09:39	11:59:46	11:57:04	12:06:23
12	12:21:26	12:27:18	12:22:45	12:13:48	12:09:24	12:12:56	12:18:43	12:18:04	12:09:18	11:59:30	11:57:11	12:06:51
13	12:21:49	12:27:17	12:22:29	12:13:33	12:09:24	12:13:08	12:18:50	12:17:53	12:08:57	11:59:16	11:57:19	12:07:19
14	12:22:11	12:27:15	12:22:12	12:13:18	12:09:24	12:13:21	12:18:56	12:17:42	12:08:36	11:59:01	11:57:29	12:07:48
15	12:22:32	12:27:12	12:21:55	12:13:03	12:09:24	12:13:34	12:19:03	12:17:31	12:08:15	11:58:48	11:57:39	12:08:16
16	12:22:53	12:27:08	12:21:38	12:12:49	12:09:25	12:13:47	12:19:08	12:17:18	12:07:53	11:58:35	11:57:50	12:08:45
17	12:23:13	12:27:04	12:21:21	12:12:35	12:09:27	12:14:00	12:19:13	12:17:06	12:07:32	11:58:22	11:58:01	12:09:15
18	12:23:32	12:26:59	12:21:04	12:12:22	12:09:29	12:14:13	12:19:18	12:16:52	12:07:10	11:58:10	11:58:14	12:09:44
19	12:23:51	12:26:53	12:20:46	12:12:09	12:09:32	12:14:26	12:19:22	12:16:39	12:06:49	11:57:59	11:58:27	12:10:14
20	12:24:08	12:26:47	12:20:28	12:11:56	12:09:35	12:14:39	12:19:26	12:16:24	12:06:28	11:57:48	11:58:42	12:10:43
21	12:24:26	12:26:40	12:20:10	12:11:44	12:09:39	12:14:52	12:19:29	12:16:10	12:06:06	11:57:38	11:58:57	12:11:13
22	12:24:42	12:26:32	12:19:52	12:11:32	12:09:44	12:15:05	12:19:31	12:15:55	12:05:45	11:57:29	11:59:12	12:11:43
23	12:24:57	12:26:24	12:19:34	12:11:21	12:09:49	12:15:18	12:19:33	12:15:39	12:05:24	11:57:20	11:59:29	12:12:13
24	12:25:12	12:26:15	12:19:16	12:11:10	12:09:54	12:15:31	12:19:34	12:15:23	12:05:03	11:57:12	11:59:47	12:12:42
25	12:25:26	12:26:06	12:18:58	12:11:00	12:10:00	12:15:43	12:19:35	12:15:07	12:04:42	11:57:05	12:00:05	12:13:12
26	12:25:39	12:25:56	12:18:40	12:10:50	12:10:06	12:15:56	12:19:35	12:14:50	12:04:22	11:56:59	12:00:24	12:13:42
27	12:25:52	12:25:45	12:18:22	12:10:40	12:10:13	12:16:08	12:19:34	12:14:33	12:04:01	11:56:53	12:00:43	12:14:11
28	12:26:03	12:25:34	12:18:04	12:10:32	12:10:21	12:16:21	12:19:33	12:14:15	12:03:41	11:56:48	12:01:04	12:14:40
29	12:26:14		12:17:46	12:10:23	12:10:28	12:16:33	12:19:32	12:13:57	12:03:21	11:56:44	12:01:25	12:15:10
30	12:26:24		12:17:28	12:10:15	12:10:37	12:16:45	12:19:29	12:13:39	12:03:01	11:56:40	12:01:46	12:15:38
31	12:26:33		12:17:10		12:10:45		12:19:26	12:13:20		11:56:38		12:16:07

Annex B


0.19
0.185
0.18
0.175
0.17
dimensionless
January
February
March
April
May
June
July
August
September
October
November
December

Annex C

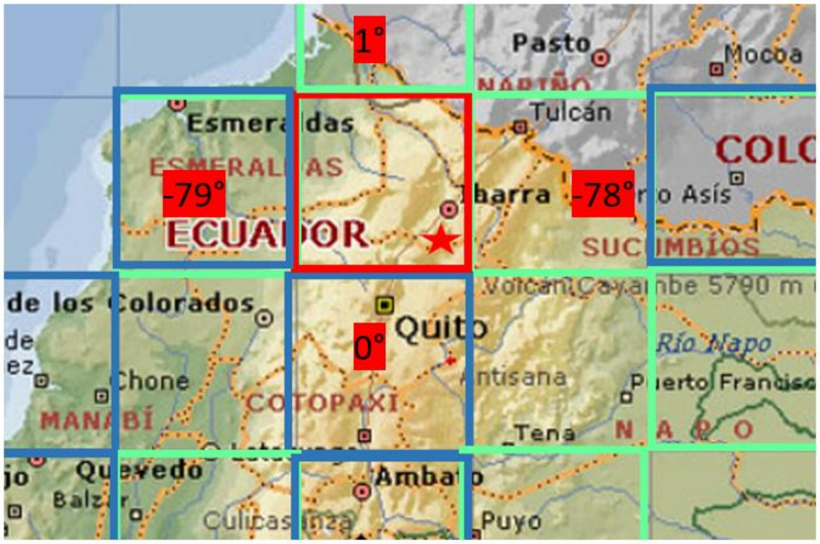

Annex D

Time Series, Area-Averaged of Ozone Total Column (Daytime/Ascending, AIRS-only) daily 1 deg. [AIRS AIRS3STD v7.0] DU over 2010-01-01 - 2020-12-31, Region 79W, 0N, 78W, 1N

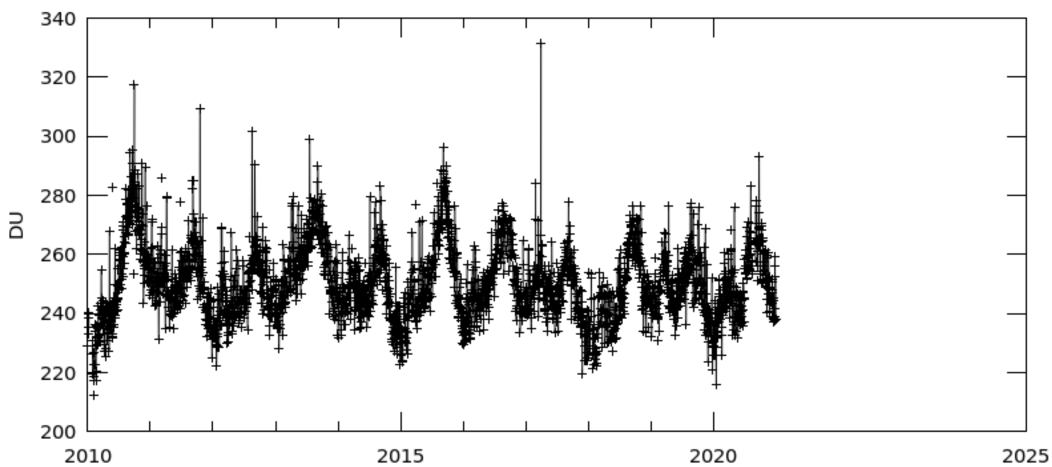

- The user-selected region was defined by 79W, 0N, 78W, 1N. The data grid also limits the analyzable region to the this point: 79W, 0N. This analyzable region indicates the spatial limits of the subsetted granules that went into making this visualization result.

Annex E

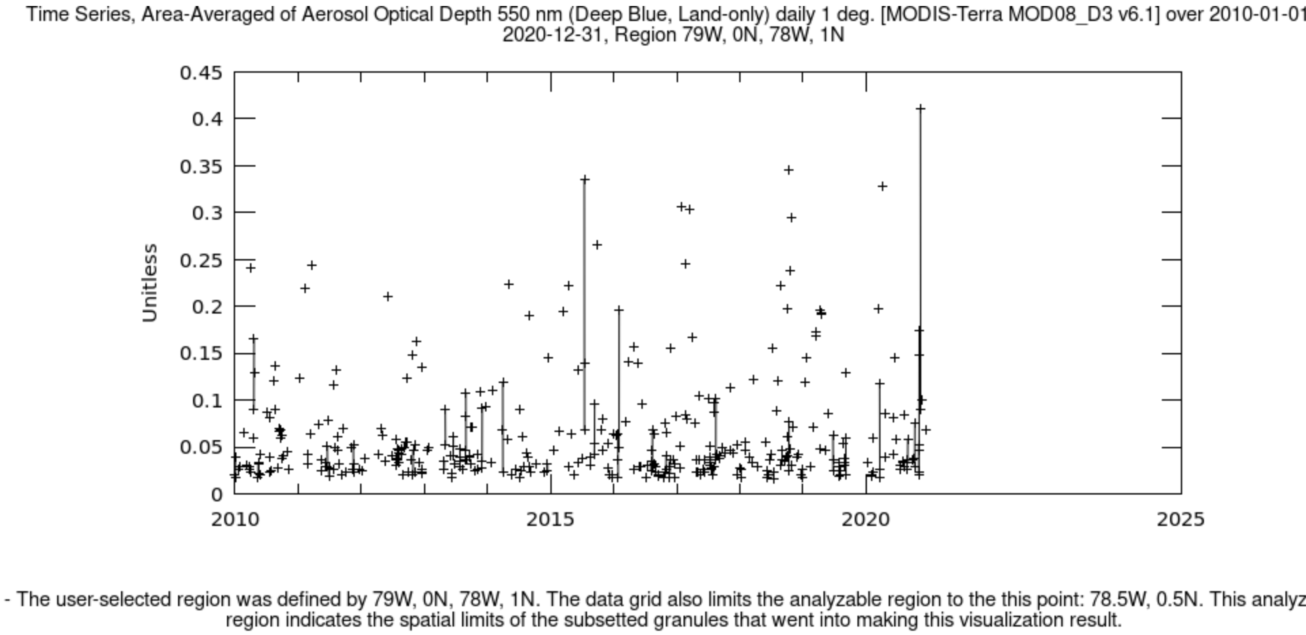

Annex F

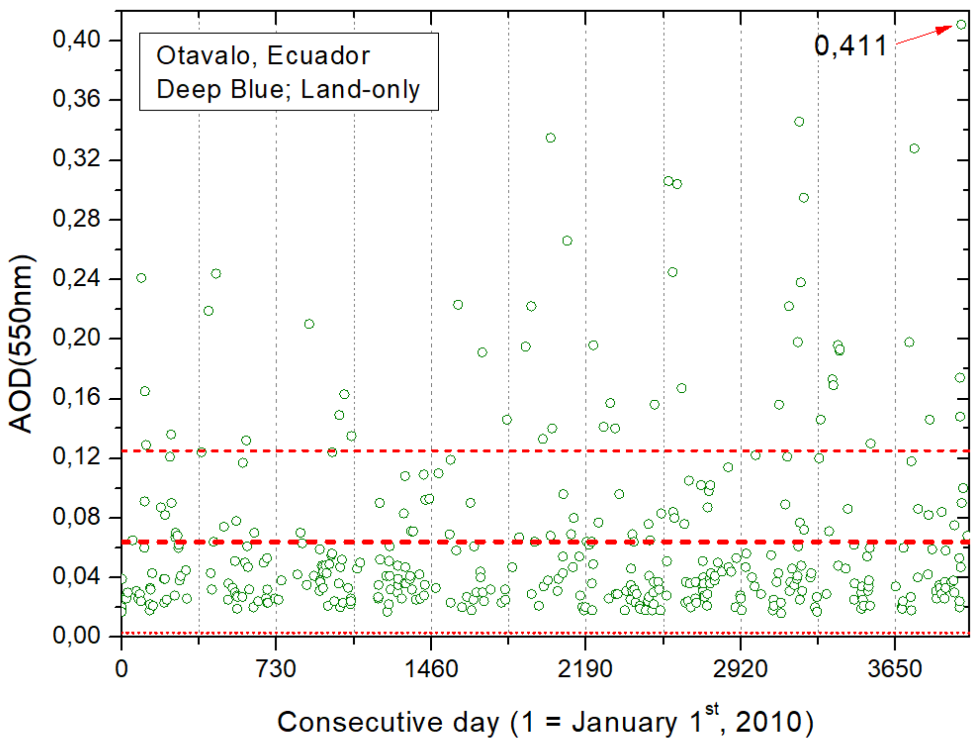

Annex G

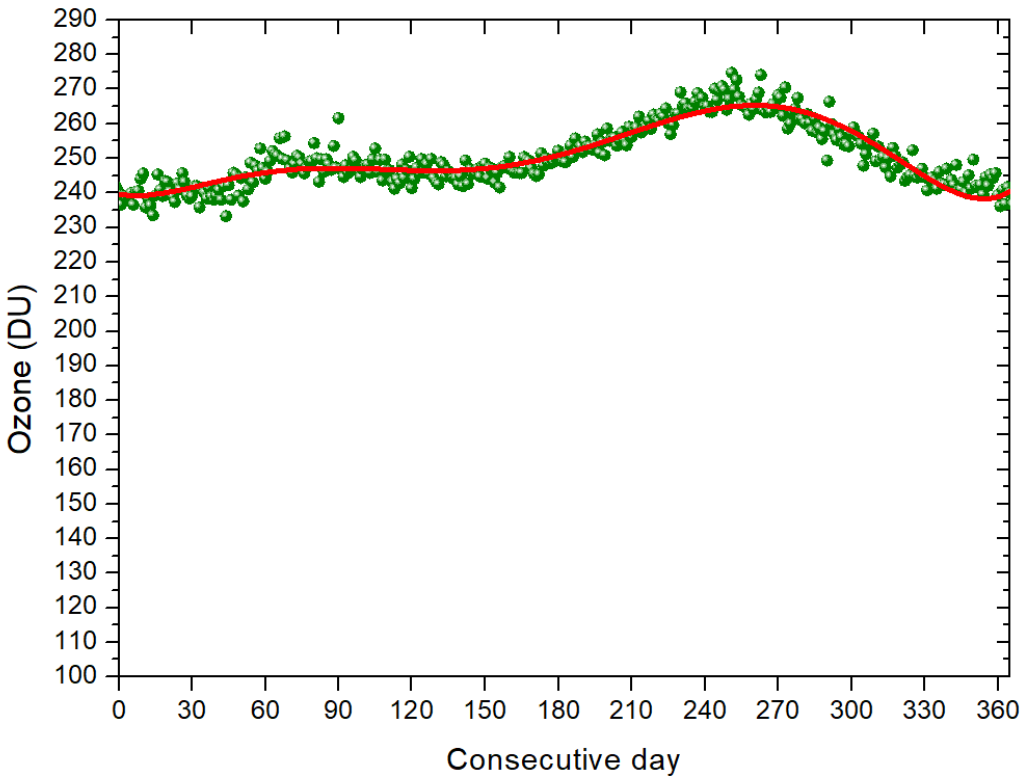

Ozone (DU)
290
280
270
260
250
240
230
220
210
200
190
180
170
160
150
140
130
120
110
100
0
30
60
90
120
150
180
210
240
270
300
330
360
Consecutive day